

ผลของการทำไฮโดรเทอร์มอลทรีตเมนต์ต่อสมรรถนะของเส้นใยนาโนของสังกะสีออกไซด์/พอลิอะครีโล  
ไนไตรล์แบบยืดหยุ่นสำหรับการกำจัดไอโทลูอิน



นายวุฒิชัย มาน้อย

จุฬาลงกรณ์มหาวิทยาลัย

CHULALONGKORN UNIVERSITY

บทคัดย่อและแฟ้มข้อมูลฉบับเต็มของวิทยานิพนธ์ตั้งแต่ปีการศึกษา 2554 ที่ให้บริการในคลังปัญญาจุฬาฯ (CUIR)  
เป็นแฟ้มข้อมูลของนิสิตเจ้าของวิทยานิพนธ์ ที่ส่งผ่านทางบัณฑิตวิทยาลัย

The abstract and full text of theses from the academic year 2011 in Chulalongkorn University Intellectual Repository (CUIR)  
are the thesis authors' files submitted through the University Graduate School.

วิทยานิพนธ์นี้เป็นส่วนหนึ่งของการศึกษาตามหลักสูตรปริญญาวิศวกรรมศาสตรมหาบัณฑิต

สาขาวิชาวิศวกรรมเคมี ภาควิชาวิศวกรรมเคมี

คณะวิศวกรรมศาสตร์ จุฬาลงกรณ์มหาวิทยาลัย

ปีการศึกษา 2559

ลิขสิทธิ์ของจุฬาลงกรณ์มหาวิทยาลัย

Effects of hydrothermal treatment on performance of flexible ZnO/PAN nanofibers for  
toluene vapor removal

Mr. Wuttichai Manoi



A Thesis Submitted in Partial Fulfillment of the Requirements  
for the Degree of Master of Engineering Program in Chemical Engineering

Department of Chemical Engineering

Faculty of Engineering

Chulalongkorn University

Academic Year 2016

Copyright of Chulalongkorn University

Thesis Title	Effects of hydrothermal treatment on performance of flexible ZnO/PAN nanofibers for toluene vapor removal
By	Mr. Wuttichai Manoi
Field of Study	Chemical Engineering
Thesis Advisor	Associate Professor Tawatchai Charinpanitkul, D.Eng.
Thesis Co-Advisor	Associate Professor Varong Pavarajarn, Ph.D.

---

Accepted by the Faculty of Engineering, Chulalongkorn University in Partial Fulfillment of the Requirements for the Master's Degree

.....Dean of the Faculty of Engineering  
(Associate Professor Supot Teachavorasinskun, D.Eng.)

THESIS COMMITTEE

.....Chairman  
(Professor Siriporn Damrongsakkul, Ph.D.)

.....Thesis Advisor  
(Associate Professor Tawatchai Charinpanitkul, D.Eng.)

.....Thesis Co-Advisor  
(Associate Professor Varong Pavarajarn, Ph.D.)

.....Examiner  
(Paravee Vas-Umnuay, Ph.D.)

.....External Examiner  
(Pamornrat Chantam, D.Eng.)

วุฒิชัย มาน้อย : ผลของการทำไฮโดรเทอร์มอลทรีตเมนต์ต่อสมรรถนะของเส้นใยนาโนของสังกะสีออกไซด์/พอลิอะคริโลไนไตรล์แบบยืดหยุ่นสำหรับการกำจัดไอโทลูอีน (Effects of hydrothermal treatment on performance of flexible ZnO/PAN nanofibers for toluene vapor removal) อ.ที่ปรึกษาวิทยานิพนธ์หลัก: รศ. ดร.ธวัชชัย ชรินพาณิชกุล, อ.ที่ปรึกษาวิทยานิพนธ์ร่วม: รศ. ดร.วรงค์ ปวรอาจารย์, 86 หน้า.

เส้นใยพอลิอะคริโลไนไตรล์ที่ตกแต่งด้วยอนุภาคนาโนรอดของสังกะสีออกไซด์ถูกเตรียมขึ้นด้วยเทคนิคการปั่นเส้นใยด้วยไฟฟ้าสถิตร่วมกับการทำไฮโดรเทอร์มอลทรีตเมนต์ สารแขวนลอยของอนุภาคสังกะสีออกไซด์ขนาด 20 นาโนเมตรในสารละลายพอลิอะคริไนไตรล์ที่ถูกละลายด้วยไตรเมทิลฟออร์มาไมด์ถูกนำไปปั่นเป็นเส้นใยด้วยเทคนิคการปั่นเส้นใยด้วยไฟฟ้าสถิต ได้เป็นเส้นใยคอมโพสิตของพอลิอะคริโลไนไตรล์และสังกะสีออกไซด์ที่มีขนาดเส้นผ่านศูนย์กลางเฉลี่ย 317 นาโนเมตร อนุภาคสังกะสีออกไซด์บนเส้นใยพอลิอะคริโลไนไตรล์ทำหน้าที่เป็นพื้นที่สำหรับการโตของอนุภาคนาโนรอดของสังกะสีออกไซด์ เส้นใยคอมโพสิตของพอลิอะคริโลไนไตรล์และสังกะสีออกไซด์ถูกนำไปผ่านกระบวนการไฮโดรเทอร์มอลทรีตเมนต์ในสถานะที่บรรจุสารละลายของสังกะสีอะซีเตทและเฮกซะเมทิลินเตตระมีนในน้ำ ทำให้เกิดอนุภาคนาโนรอดของสังกะสีออกไซด์บนเส้นใยพอลิอะคริโลไนไตรล์ นอกจากนี้ยังได้ศึกษาอิทธิพลของความเข้มข้นของสังกะสีอะซีเตท อุณหภูมิและเวลาในการทำไฮโดรเทอร์มอลทรีตเมนต์ และสัดส่วนของสังกะสีอะซีเตทต่อเฮกซะเมทิลินเตตระมีน นอกจากนี้ยังพบว่าเส้นใยที่ผ่านกระบวนการไฮโดรเทอร์มอลทรีตเมนต์ยังคงความยืดหยุ่นไว้ได้อย่างดี เส้นใยนาโนของสังกะสีออกไซด์/พอลิอะคริโลไนไตรล์ถูกนำมาทดสอบสมรรถนะในการกำจัดสารอินทรีย์ระเหยง่ายโดยอาศัยการเร่งปฏิกิริยาโดยใช้แสง โดยใช้โทลูอีนเป็นตัวแทนของสารอินทรีย์ระเหยง่าย พบว่าโทลูอีนสามารถถูกกำจัดได้กว่า 95% ภายในเวลา 2 ชั่วโมง

ภาควิชา วิศวกรรมเคมี

ลายมือชื่อนิสิต .....

สาขาวิชา วิศวกรรมเคมี

ลายมือชื่อ อ.ที่ปรึกษาหลัก .....

ปีการศึกษา 2559

ลายมือชื่อ อ.ที่ปรึกษาร่วม .....

# # 5770563521 : MAJOR CHEMICAL ENGINEERING

KEYWORDS: ZINC OXIDE, NANOFIBER, ELECTROSPINNING, HYDROTHERMAL, PHOTOCATALYSIS, VOLATILE ORGANIC COMPOUNDS

WUTTICHAJ MANOI: Effects of hydrothermal treatment on performance of flexible ZnO/PAN nanofibers for toluene vapor removal. ADVISOR: ASSOC. PROF. TAWATCHAI CHARINPANITKUL, D.Eng., CO-ADVISOR: ASSOC. PROF. VARONG PAVARAJARN, Ph.D., 86 pp.

Polyacrylonitrile nanofibers decorated by zinc oxide nanorods were fabricated by combination of electrospinning technique and hydrothermal treatment. Suspension of 20 nm ZnO nanoparticles in PAN solution was subjected to electrospinning technique. The composite nanofibers of ZnO and PAN in the average diameter of 317 nm were obtained. The ZnO nanoparticles on the surface of PAN nanofibers act as nucleation sites for growth of ZnO nanorods. The obtained ZnO/PAN nanofibers were subjected to hydrothermal treatment process using the autoclave containing solution of zinc acetate and hexamethylenetetramine in water. The ZnO nanorods formed on the surface of PAN nanofibers. In addition, influence of zinc acetate concentration, treatment temperature, treatment time, and zinc acetate : hexamethylenetetramine ratio were also studied. It was also found that the obtained ZnO/PAN nanofibers still possess flexibility. The ZnO/PAN nanofibers were subjected to investigate performance of VOCs removal using photocatalytic reaction. Toluene was used as delegate for VOCs. It was found that the gaseous toluene could be degraded for more than 95% within 2 hours.

Department: Chemical Engineering	Student's Signature .....
Field of Study: Chemical Engineering	Advisor's Signature .....
Academic Year: 2016	Co-Advisor's Signature .....

## ACKNOWLEDGEMENTS

I am very thankful to thesis advisor and co-advisor, Associate Professor Dr. Tawatchai Charinpanitkul and Associate Professor Dr. Varong Pavarajarn Department of Chemical Engineering, Chulalongkorn University for encouragement and suggestion through academic program. Moreover, I am also thankful to Prof. Dr. Siriporn Damrongsakkul, Dr. Paravee Vas-Umnuay, and Dr. Pamornrat Chantam for their comments and participation,

This work was partially supported by The Silver Jubilee Fund of Chulalongkorn University through The Climate Change and Disaster Management Research Cluster (CU 56-357-CC).

Finally, I would like to thank to Center of Excellence in Particle Technology (CEPT), Department of Chemical Engineering, Faculty of Engineering, Chulalongkorn University for serving place and equipment. The most of graduation is devoted to my family.

## CONTENTS

	Page
THAI ABSTRACT .....	iv
ENGLISH ABSTRACT .....	v
ACKNOWLEDGEMENTS .....	vi
CONTENTS .....	vii
LIST OF TABLE .....	ix
LIST OF FIGURE.....	x
Chapter 1.....	1
Introduction .....	1
1.1 Motivation.....	2
1.2 Objective of research .....	4
1.3 Scopes of research.....	5
Chapter 2.....	6
Fundamental and Literature reviews.....	6
2.1 Volatile organic compounds (VOCs).....	6
2.2 Photocatalysis .....	10
2.3 Zinc oxide (ZnO).....	14
2.5 Electrospinning.....	19
2.6 Polyacrylonitrile (PAN).....	22
2.7 Literature reviews.....	24
Chapter 3.....	30
Experiment.....	30
3.1 Materials.....	30

	Page
3.2 Preparation of ZnO nanostructure/PAN nanofibers .....	30
3.3 Characterization .....	34
3.4 Photocatalytic degradation process .....	35
Chapter IV.....	37
Results and Discussion .....	37
4.1 Fabrication of flexible ZnO/PAN nanofibers .....	37
4.1.1 Effect of zinc acetate concentration .....	40
4.1.2 Effect of temperature .....	44
4.1.3 Effect of treatment time .....	48
4.1.4 Effect of zinc acetate:HMT ratio .....	53
4.2 Mechanical properties of ZnO/PAN nanofibers .....	54
4.3 Photocatalytic VOC degradation .....	58
Chapter V.....	68
Conclusion .....	68
5.1 Summary of results.....	68
5.2. Conclusion.....	69
REFERENCES .....	71
APPENDIX.....	75
VITA.....	86



## LIST OF TABLE

Table	Page
Table 1. chemical structures and sources of curtain indoor VOCs .....	8
Table 2. properties of wurtzite ZnO .....	16
Table 3. summary of hydrothermal parameter ranges. ....	28
Table 4. residual Zn contents in the autoclave after hydrothermal treatment at various temperatures.....	48
Table 5. residual Zn contents in the autoclave after hydrothermal treatment for various treatment times.....	41
Table 6. specific surface areas of various nanofibers.....	52
Table 7. aspect ratios of ZnO nanorods prepared by various zinc acetate concentrations.....	65
Table 8. aspect ratios of ZnO nanorods prepared by various hydrothermal temperatures .....	67

## LIST OF FIGURE

<b>Figure</b>	<b>Page</b>
Fig. 1 indoor and outdoor level of VOCs in office building in Bangkok .....	7
Fig. 2 safety sign of toluene in NFPA system.....	10
Fig. 3 electronic state of metal, semiconductor and insulator.....	11
Fig. 4 schematic of semiconductor and photocatalytic mechanism .....	11
Fig. 5 band positions of several semiconductors .....	14
Fig. 6 ZnO crystal structures.....	15
Fig. 7 schematic of autoclave reactor .....	18
Fig. 8 pressure-temperature diagram for various filling degree of pure water.....	19
Fig. 9 schematic of electrospinning process .....	20
Fig. 10 schematic of application field targeted by patents on electrospun nanofibers .....	22
Fig. 11 chemical structure of polyacrylonitrile repeat unit.....	23
Fig. 12 schematic of electrospinning process.....	32
Fig. 13 autoclave reactor.....	33
Fig. 14 condition of hydrothermal experiment diagram.....	33
Fig. 15 photograph of photoreactor.....	35
Fig. 16 SEM images (a, c) and diameter size distribution (b, d) of PAN and ZnO seeds/PAN nanofibers.....	39
Fig.17 SEM images of hydrothermalized ZnO/PAN nanofibers from various zinc acetate concentration .....	40
Fig. 18 diameter and length of ZnO nanorods prepared by various zinc acetate concentration .....	43
Fig. 19 percent of increased weight of fibers after hydrothermal process of various zinc acetate concentration.....	44
Fig. 20 SEM image of ZnO/PAN nanofibers prepared by various temperatures .....	45
Fig. 21 average diameter and length of ZnO nanorods prepared by various temperatures .....	46

Fig. 22 percentage of increased weight of fibers after hydrothermal treatment at various temperatures.....	47
Fig. 23 SEM images of ZnO/PAN nanofibers prepared by various treatment times. ....	49
Fig. 24 average diameters and lengths of ZnO/PAN nanofibers prepared by various treatment times.....	50
Fig. 25 percent of increased weight of fibers after hydrothermal treatment for various treatment times.....	51
Fig. 26 average diameter of various fibers.....	53
Fig. 27 SEM images of ZnO/PAN nanofibers prepared by various zinc acetate:HMT ratio.....	54
Fig. 28 photograph of bending of ZnO/PAN nanofibers after hydrothermal treatment.....	55
Fig. 29 stress-strain curve of various ZnO/PAN nanofibers . ....	57
Fig. 30 modulus of ZnO/PAN nanofibers before and after hydrothermal treatment at various temperatures.....	57
Fig. 31 Toluene removal by various photocatalysts. ....	61
Fig. 32 photocatalytic degradation of toluene in batch reactor by ZnO/PAN nanofibers before and after hydrothermal treatment.....	63
Fig. 33 Plot of $\ln 1/(1-X)$ against reaction time.....	63
Fig. 34 photocatalytic degradation of toluene in batch reactor by ZnO/PAN nanofibers prepared by various zinc acetate concentration. ....	64
Fig. 35 photocatalytic degradation of toluene in batch reactor by ZnO/PAN nanofibers prepared by various hydrothermal temperatures.....	66
Fig. 36 photocatalytic degradation of toluene in batch reactor by ZnO/PAN nanofibers prepared by various treatment times. ....	67
Fig. 37 SEM images of ZnO/PAN nanofibers prepared by various zinc acetate concentrations.....	73
Fig. 38 SEM images of ZnO/PAN nanofibers prepared by various treatment temperatures.....	74
Fig. 39 SEM images of ZnO/PAN nanofibers prepared by various treatment time.....	75

Fig. 40 diameter size distribution of ZnO nanorods prepared by various zincacetate concentrations.....	76
Fig. 41 diameter size distribution of ZnO nanorods prepared by treatment temperatures .....	77
Fig. 42 diameter size distribution of ZnO nanorods prepared by treatment times .....	78
Fig. 43 length size distribution of ZnO nanorods prepared by various zincacetate concentrations.....	89
Fig. 44 length size distribution of ZnO nanorods prepared by treatment temperatures.....	80
Fig. 45 length size distribution of ZnO nanorods prepared by treatment times. ....	81
Fig. 46 XRD pattern of PAN and ZnO/PAN nanofibers .....	82
Fig. 47 TGA curve of PAN and ZnO/PAN nanofibers.....	82



## Chapter 1

### Introduction

Remediation of indoor air pollution including volatile organic compounds (VOCs) as a major air pollutant has been an environmental concern for a long period because VOCs can be the long-term risk on human health. Exposure to VOCs could result in headache, sore throat, stinging eyes, fatigue respiration problems and other effects on human being. World Health Organization (WHO) has indicated these symptoms as sick building syndrome [1]. It has been recognized that VOCs can be released from daily consumable products, such as painting, perfumes, floor cleaner, printer, adhesive materials and tobacco. Indoor air management by mean of good ventilating indoor air and eliminating released VOCs has been employed as typical practice so far. However, there are still some disadvantages of such methods, such as adsorption, biofiltration, and direct combustion [2]. As a result, there are requirements of new technologies which could overcome those problems. In this thesis, some issues related to integration of photocatalyst and nanofiber preparation have been explored for figuring out an academic motivation which will be deliberated later.

## 1.1 Motivation

Meanwhile, photocatalytic oxidation technique for eliminating organic compounds has been developed by many research teams because of their cost-effective, high efficiency, and environmental friendly. Photocatalytic oxidation could degrade VOCs to water and carbon dioxide ( $\text{CO}_2$ ) by making use of UV illuminated photocatalysts. Such photocatalysts are usually semi-conductive metal oxides, such as ZnO,  $\text{TiO}_2$ , and  $\text{WO}_3$  [1-3]. Among those photocatalysts, Zinc Oxide (ZnO) has been considered as a promising candidate because of its wide band gap, economical cost, non-toxicity, and environmental friendliness. It should be noted that ZnO is usually in a form of powder, resulting in limitation for practical application, such as difficulty in handling. There are some novel ideas to fabricate ZnO in a form of nanofibers to overcome such limitation. Among those ideas, electrospinning is recognized as one of the simple methods for preparing inorganic nanofibers. Such nano-fibrous structure possesses high surface-to-volume ratio, resulting in large exposure area which is required for photocatalytic reaction. Electrospinning technique relies on electrical force to draw viscous liquid to fiber form, which could prepare inorganic compounds nanofibers, such as ZnO and  $\text{TiO}_2$  nanofibers by spinning fiber from a solution of such inorganic precursor in polymer. The as-spun fibers would be subjected to calcination at high temperature for converting to

inorganic nanofibers [4-7]. However, such nanofibers of those inorganic compounds would suffer with a main drawback of their brittleness.

Because of polymer within composite nanofibers, the fiber can retain its flexibility. Many researchers have been attempting to fabricate flexible metal oxide nanofibers using various methods. For example, photocatalyst nanoparticles could be dispersed in a polymer solution and the suspension is then electrospun into composite nanofibers [8]. Another method, polymer nanofibers were immersed in a sol-gel solution to deposit metal oxide on the surface of the nanofibers [9]. However, for these methods, the photocatalyst nanoparticles would agglomerate and cover unevenly over the surface of fibers. These problem can be overcome by mean of firstly prepare composite metal oxide precursor/polymer nanofibers and were subsequently subjected to hydrothermal at moderate temperature and therefore metal oxide nanoparticle in polymer fibers were obtained. In addition, the fibers still retain flexibility [10, 11].

Hydrothermal technique can synthesize inorganic particles with various morphology such as nanorods, nanowires, nanoparticles, nanoflakes, and other [12-16]. ZnO nanorods and nanowires can be synthesized by hydrothermal method. Moreover, ZnO nanorods and nanowires can be arrayed to obtain aligned nanorods by supplying seed layers to allow ZnO grow on the seed layers [17-20]. Fortunately, ZnO nanorods could be decorated on the surface of polymer nanofibers by firstly coat ZnO seeds on the surface of polymer nanofibers and subject to hydrothermal

treatment later. To obtain ZnO nanowires or nanorods uniformly decorate on the surface of nanofibers, the nanofibers should be supplied seeds. There are many methods to coat ZnO seeds layers on the surface of substrate such as radio frequency (RF) sputtering, atomic layer deposition (ALD), pulse layer deposition (PLD), and so on [17-19, 21]. These methods are high-cost technology. This work prepared ZnO seeds on the surface of polymer nanofibers by facile method.

Hydrothermal method would lead to polyacrylonitrile nanofibers incorporated intimately with ZnO nanorods. It should be noted that the composite fibers would not be seriously damaged and still retain flexibility. Therefore, flexibility of ZnO/polymer obtained by hydrothermal treatment should be confirmed. However, effect of hydrothermal parameters such as temperature, treatment time, concentration of Zn precursor, and Zn precursor/alkali source ratio need to be investigated.

In this work, PAN nanofibers decorated with ZnO nanorods will be used for photocatalytic degradation of gas-phase toluene, which toluene is used as model VOCs. Finally the performance of ZnO/PAN nanofibers for toluene removal would be examined with regard to their preparing conditions.

## 1.2 Objective of research

To study on effects of temperature, treatment time, concentration of zinc acetate, and zinc acetate/hexamethylenetetramine ratio in hydrothermal treatment on performance of ZnO/PAN nanofibers for gas-phase toluene removal.



### 1.3 Scopes of research

1.3.1 Synthesize PAN nanofibers embedded ZnO seeds using electrospinning by controlling PAN concentration, amount of ZnO, voltage, distance between needle and collector, and flow rate based on previous works.

1.3.2 Synthesize PAN nanofibers decorated ZnO nanorods using hydrothermal method by varying temperature, treatment time, concentration of zinc acetate, and zinc acetate/HMT ratio.

1.3.3 Investigate photocatalytic degradation of gas-phase toluene using fabricated ZnO/PAN nanofibers under designed condition.

1.3.4 Characterize the fabricated ZnO/PAN nanofibers as well as detect toluene concentration by following instruments;

- Scanning Electron Microscope (SEM)
- Atomic Adsorption Spectroscopy (AAS)
- The Brunauer-Emmett-Teller (BET)
- Universal Testing Machine
- Gas chromatography (GC)

## Chapter 2

### Fundamental and Literature reviews

This chapter is composed of 2 main sections; section 1 is related to fundamental knowledges, which involve with volatile organic compounds (VOCs), photocatalyst, zinc oxide (ZnO), electrospinning technique and hydrothermal method. Section 2 is literature review, which survey previous studies.

#### 2.1 Volatile organic compounds (VOCs)

VOCs are the pollutant in form of gases and volatile substance under the ambient temperature and humidity condition. Such VOCs consist of carbon atoms and other atoms such as hydrogen and. There are such groups of VOCs, such as aliphatic hydrocarbon, aromatic hydrocarbon, halogenated hydrocarbons and oxygenated hydrocarbon.

##### 2.1.1 Indoor VOCs

Concentration of indoor VOCs is 5-10 times higher than that of outdoor times because of their ventilation. As a result, concern in such indoor VOCs is more important than the outdoor VOCs. Generally, there are types of indoor VOCs more than 300 types. Each type is released from different sources. Ongwandee et al (2011) [22] investigated concentration of VOCs in office building in Bangkok as shown in Fig. 1 The results shown that the VOC concentration varied among the building.

The two most remarkable VOCs were toluene and limonene with average concentrations of 110 and 60.5  $\mu\text{g}/\text{m}^3$ , respectively. Moreover, the results indicate that the indoor VOCs are higher than outdoor concentrations. The concentration of indoor VOCs depends on several factors such as ventilation system, temperature, VOCs source, humidity, latest building decoration and human activity.

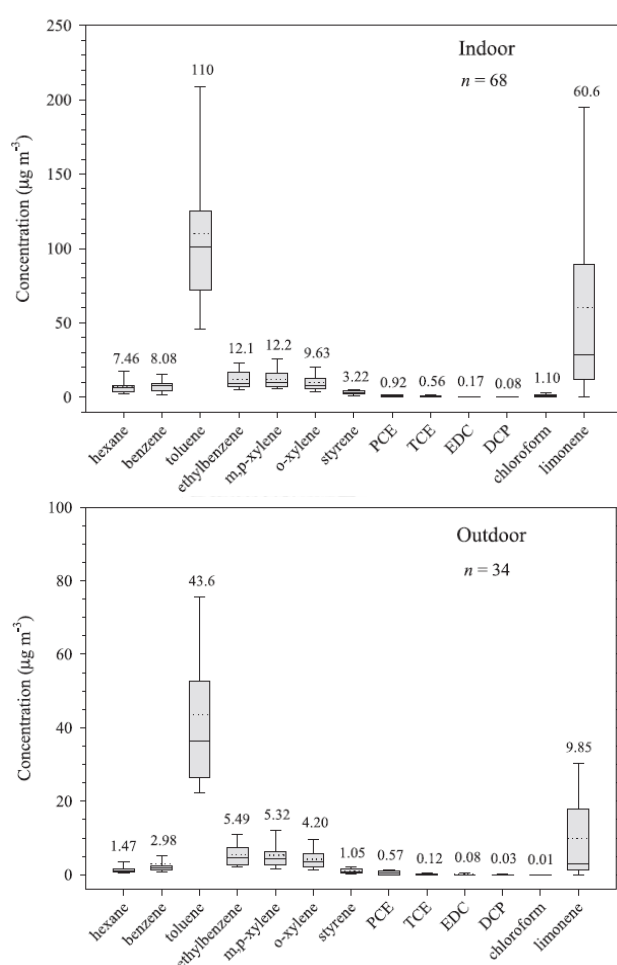
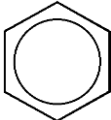
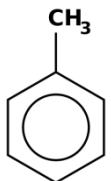
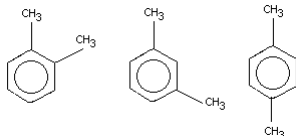
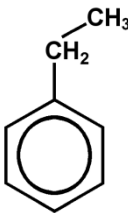
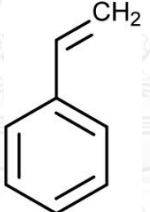
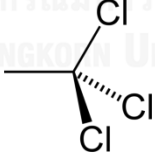
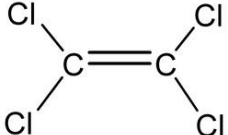
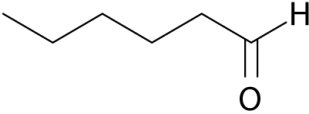
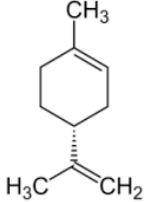


Fig. 1 indoor and outdoor level of VOCs in office building in Bangkok [22]

Indoor VOCs is usually released from paints, wallpaper, office equipment (printer, photocopier, computer, and so on) cleaning product, and so on. The Types of VOCs released in indoor environment and chemical structure was demonstrated in Table 1 As well as the source of these VOCs also demonstrated.

Table 1. chemical structures and sources of curtain indoor VOCs

Types of VOCs	Chemical structure	Sources
benzene		paints, binder in particle broad, tobacco smoke
toluene		paint, binder in particle broad, tobacco smoke
xylene		solvent
ethylbenzene		paints, solvent
styrene		insulator, photocopier, paints, plastic
trichloroethane		ink, paints, solvent
tetrachloroethylene		cleaning product
hexanal		paints, mirror
limonene		fragrant and cleaning product

Toluene is mostly found in office building in Thailand as shown in Fig.

1.1 Therefore, toluene will be chosen as model VOCs for this work.

### 2.1.2 Toluene

Toluene, methylbenzene,  $C_7H_8$ , is colorless, flammable liquid of low viscosity with benzene-like odor. It is miscible with most organic solvent such as alcohol, ketone, phenols, esters, and chlorohydrocarbons. Toluene is slightly soluble in water, 0.4 g/100 ml at  $15^\circ C$ . Toluene own some their physical properties such as 92.13 g/mol of molecular mass,  $-94.991^\circ C$  of melting point, and  $110.625^\circ C$  of boiling point [23]. Toluene is usually used as a component in paints. In addition, toluene vapor is also found in tobacco smoke.

Toluene is considered as toxic substance. Material Safety Data Sheet (MSDS) of toluene shown safety sign in NFPA system as level 2 in health region (blue region) as shown in Fig.2 Inhalation of toluene vapor affects the central nervous system, resulting in symptoms as headaches, dizziness, or coordination difficulties. At higher concentration, loss of consciousness can occur. In animal experiments the toxicity values were found that [23]:

Rat, oral,  $LD_{50} = 5000 \text{ mg/kg}$

Rabbit, percutaneous,  $LD_{50} = 12,124 \text{ mg/kg}$

Mouse, 8 hr inhalation,  $LD_{50} = 5320 \text{ mg/m}^3$

In prolonged exposure, toluene accumulates in the brain, resulting in chronic toxicity is occurred.

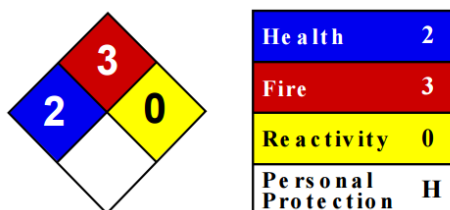


Fig. 2 safety sign of toluene in NFPA system

## 2.2 Photocatalysis

Photocatalytic process is utilized for degradation of organic compounds because of their cost-effective, high efficiency, and environmental friendly. Photocatalysis is a chemical reaction induced by photoabsorption of solid photocatalyst. The photocatalytic process was reported that organic molecules contact with surface of catalyst under irradiation, inducing oxidation and reduction reactions and degrading organic compounds to water (H<sub>2</sub>O) and carbon dioxide (CO<sub>2</sub>). The photocatalyst requires a semiconductive property due to energy band gap of the semiconductor is even wide while metal is too narrow and insulator is too wide. The energy band gap is the energy difference between conduction band and valence band. Fig.3 illustrates electronic state in metal, semiconductor and insulator.

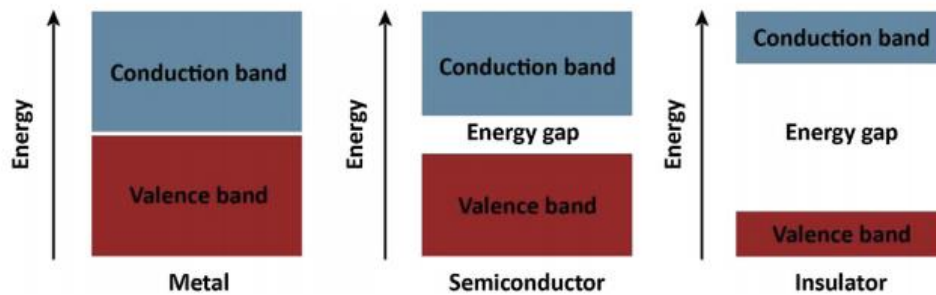


Fig. 3 electronic state of metal, semiconductor and insulator [24]

Photocatalytic process relates to two major steps: (i) light absorption and generation of electron-hole pairs; (ii) oxidation and reductions at the semiconductor surface. Once the semiconductor is irradiated with energy higher than band gap, electrons ( $e^-$ ) are excited from valence band (VB) to conduction band (CB), leaving positive holes ( $h^+$ ) at the valence band. After that excited electrons ( $e^-$ ) in the conduction band and generated hole ( $h^+$ ) in the valence band transfer to the surface of semiconductor. Fig.4 shows the schematic of semiconductor and photocatalytic mechanism.

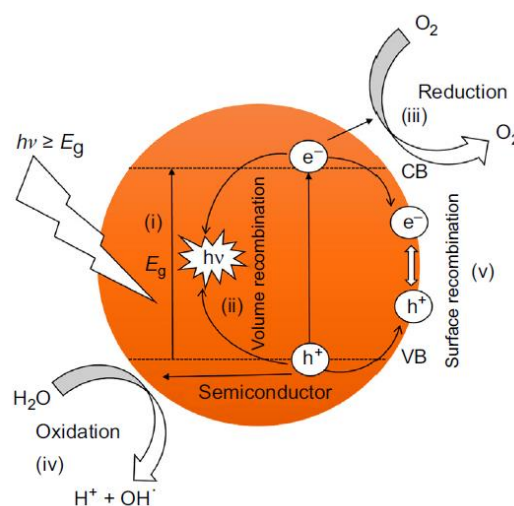
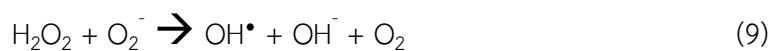
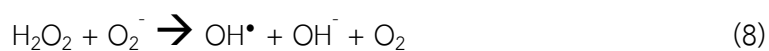
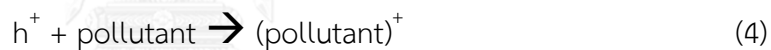
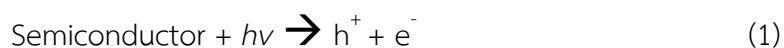


Fig. 4 schematic of semiconductor and photocatalytic mechanism [25]

Normally, the photocatalytic degradation of pollutants is accepted that consist of many of reactions after irradiation of semiconductor material. These reactions consisted electron-hole generation and degradation of pollutant through oxidation and reduction reaction [25]:







From equation (1) – (11), It is exhibited that photocatalytic process relates to a series of step reactions, which contains generation of hydroxyl radicals ( $\text{OH}^\bullet$ ). These radicals are a strong oxidizing agent which having power could degrade many organic pollutants as well as converting bioresistant substance into harmless products.

To obtain a high efficiency of photocatalytic process, the selected photocatalyst would be considered about band gap energy of semiconductor and energy level for transportation of photoelectrons. The position of valence band and conduction band are important parameters. The valence band should be lower than oxygen oxidation potential and conduction band should be higher than hydrogen reduction potential [25]. Fig.5 shows band positions of several semiconductors.

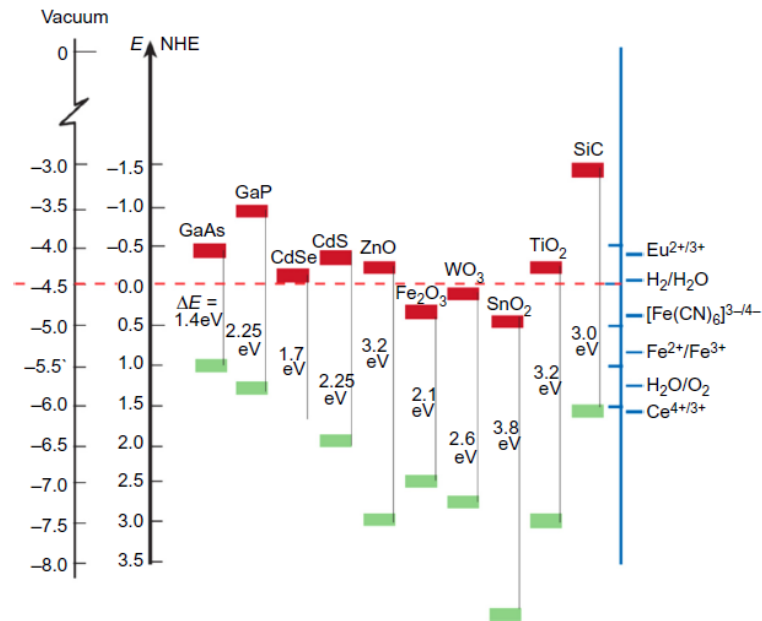


Fig. 5 band positions of several semiconductors [25]

Among those metal compounds semiconductor, ZnO possesses quite wide band gap energy as well as valence band is lower than  $\text{OH}^*/\text{H}_2\text{O}$  potential (+2.27 eV) and conduction band should be higher than  $\text{O}_2/\text{O}_2^-$  potential (-0.28 eV). Therefore, ZnO is usually used as photocatalyst.

จุฬาลงกรณ์มหาวิทยาลัย  
CHULALONGKORN UNIVERSITY

### 2.3 Zinc oxide (ZnO)

ZnO is an inorganic compound with the chemical formula "ZnO". ZnO appear as white powder, odorless. ZnO possess unique physical and chemical properties, such as low solubility in water, high chemical stability and high photostability. The crystal structures of ZnO compose of wurtzite, zinc blend, and rocksalt as schematically shown in Fig.6 Under ambient condition, ZnO is usually thermodynamically stable in structure of wurtzite. The zinc blend structure can be

stabilized only by growth on substrate of cubic lattice structure. The rocksalt structure may be occurred at high pressure [26].

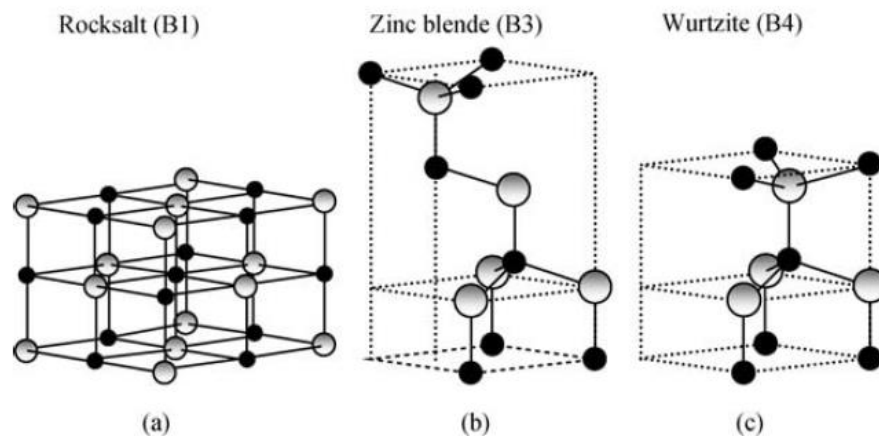


Fig. 6 ZnO crystal structures: (a) rocksalt, (b) zinc blend, and (c) wurtzite

gray ball denote Zn atom and black ball denote O atom [26]

ZnO is a semiconductor with a wide energy band gap (3.2 eV), high bond energy (60 meV), high mechanical stability and high thermal stability at ambient condition and some other properties is shown in Table 2 [27]. Because of these properties of ZnO, it is attracted for utilize in several application. The piezo- and pyroelectric properties of ZnO, it is used as sensor and photocatalyst in pollutant removal and hydrogen production. Because of hardness and rigidity, it is used as material in the ceramic industry. It is used as a material for biomedicine and in pro-ecological systems because of their low toxicity and biocompatibility [28].

Table 2. properties of wurtzite ZnO

Property	Value
Lattice parameter at 300 K	
$a_0$	0.32495 nm
$c_0$	0.52069 nm
$a_0/c_0$	1.602 (ideal hexagonal structure shows
$u$	1.633)
	0.345
Molar mass	81.38 g/mol
Density	5.606 g/cm <sup>3</sup>
Stable phase at 300 K	Wurtzite
Melting point	1,975 °C
Solubility in water	0.0004% (17.8 °C)
Thermal conductivity	0.6, 1-1.2 W/cm K
Linear expansion coefficient (1/°C)	$a_0$ : $6.5 \times 10^{-6}$ $c_0$ : $3.0 \times 10^{-6}$
Static dielectric constant	8.656
Refractive index	2.008, 2.029
Excitation binding energy	60 meV
Electron effective mass	0.24
Electron Hall mobility at 300 K	200 cm <sup>2</sup> /V s
Hole effective mass	0.59
Hole Hall mobility at 300 K	5-50 cm <sup>2</sup> /V s

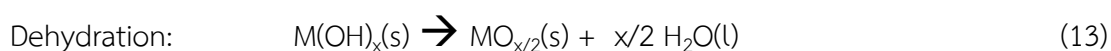
ZnO can be synthesized by variety of methods, such as vapor deposition, precipitation in water solution, precipitation from microemulsion, mechanochemical process, sol-gel process and hydrothermal process. This verity of methods makes it

possible to obtain ZnO particles with different in size, structure and shape such as nanorod, nanoparticle, nanowire, nanoflower, etc.

## 2.4 Hydrothermal technique

Several metal oxides including ZnO can be synthesized by numerous methods, such as chemical vapor deposition (CVD), sol-gel, precipitation, atomic layer deposition, hydrothermal, etc. Among these method, hydrothermal offers many advantages such as simplicity, low temperature, and low cost. Hydrothermal process is the process that is operated at high temperature (often above solvent boiling point) and pressure resulting the solvent is still liquid phase. The medium used as water the process is called “hydrothermal”, while solvent is called “solvothermal”.

The precursor used in the synthesis of metal oxides is usually aqueous solution of metal salt such as acetate, nitrate, or chloride. These salts can be converted to metal hydroxides prior to ZnO formation using a base such as sodium hydroxide (NaOH), hexamethylenetetramine (HMT), potassium hydroxides (KOH), and other. The metal hydroxide is then dehydrated to form ZnO. The two reactions that lead from metal salts to metal oxides are hydrolysis and dehydration as shown below [29]:



Where, M represents the metal and X the anion. Some parameters influenced growth of ZnO such as temperature, residence time, precursor concentration, pH, and others.

For reactors for hydrothermal synthesis, a conventional synthesis is usually operated in batch reactor. The precursor is dissolved in the solvent like water in an autoclave as reactor, which can resist high temperature and pressure. Configurations of the autoclave were shown in Fig. 7. The main components of the autoclave consisted steel shell and lid, Teflon cup is placed inside the steel shell because of their chemical stability. The precursor solution is filled in the Teflon cup.

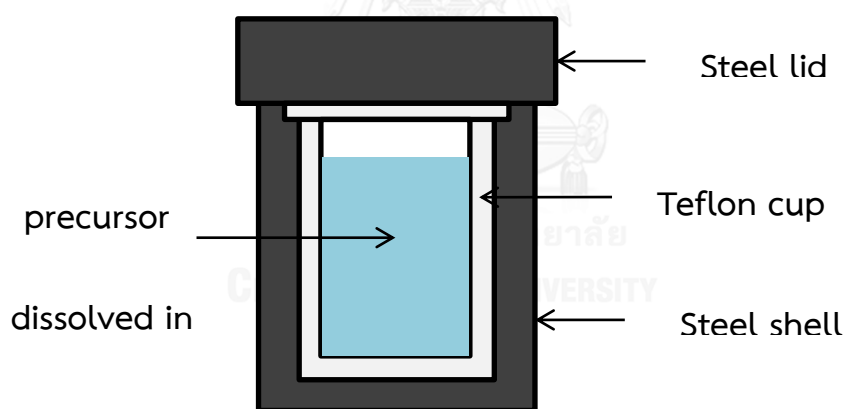


Fig. 7 schematic of autoclave reactor

The autoclave is sealed and heated up to high temperature, while the pressure is generated autogenously. The pressure depends on filling degree, pressure can be raised up to several hundred bars, even low temperature with the pressure at equilibrium. The pressure can be calculated from volume of liquid. Fig. 8 shows the

pressure-temperature diagram for various filling degree of pure water. It shows that pressure variation occurs above 150°C for filling degree of 90%. Therefore, for hydrothermal reaction, the autoclave must be material that durable to very high pressure. Moreover, hydrothermal process conducted under supercritical condition can synthesize metal oxide particle with smaller size and narrower size distribution than subcritical condition. In addition, hydrothermal process operated under supercritical water is reducing alkaline concentration for crystal phase formation. High alkalinity causes corrosion of reactor, thereby making it a problem for industrial manufacture.

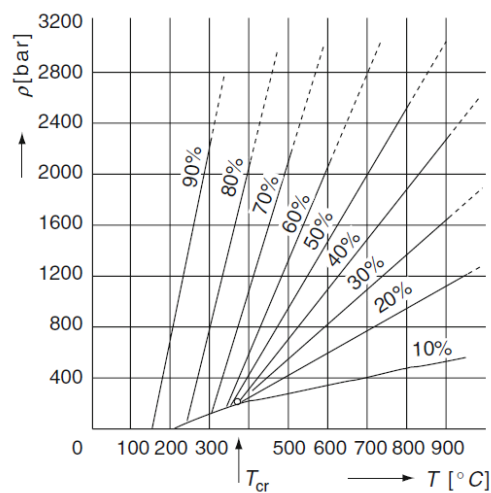


Fig. 8. pressure-temperature diagram for various filling degree of pure water [30]

## 2.5 Electrospinning

Electrospinning is a process can fabricate polymer fibers in diameters ranging from micron down to nanometer. The fibers in the nanometer diameter rang is called nanofiber. The nanofiber possesses large surface area per unit mass and small

pore size. The electrospinning uses of electrostatic process to form solid fibers from a polymeric fluid using a high-voltage electric field. Electrospinning is easily conducted by applying a high voltage (often kV level) to capillary (often syringe used), which is connected with millimeter diameter nozzle filled with polymer solution or melt to be electrospun by assistance of an electrode. As a result, the fibers are collected on a grounded target plate collector, which can be covered by fiber mats. Aluminium foil or ohther metals usually are used as a collector material. While pump is used to initiate the droplet by controlling flow rate of polymer solution. Schematic of electrospinning process is illustrated in Fig. 9.

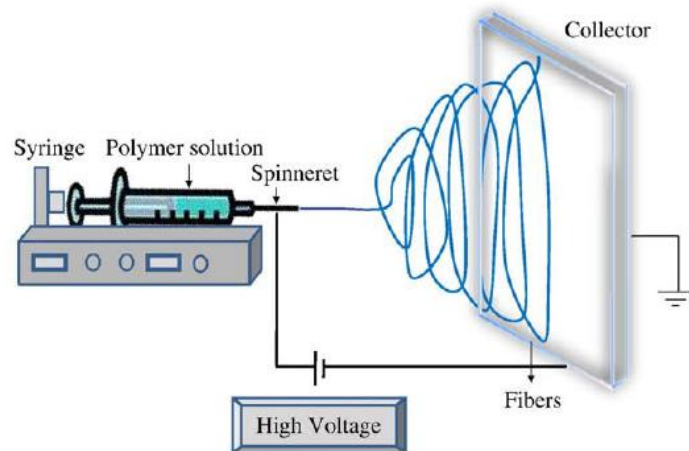


Fig. 9 schematic of electrospinning process [31]

Phenomena of the electrospinning process can be briefly described. At the end of the capillary, polymer fluid is held by surface tension. Once electric field is subjected to the end of capillary, a charge is induced on the surface of polymer fluid. Therefore, there are 2 forces at the surface of the polymer fluid, which is charge repulsion force opposite to the surface tension. As electric field intensity is



increased, the surface of polymer liquid at the end of the capillary is elongated to form a conical shape called Taylor cone. When electric field is increased, electrostatic force can overcome the surface tension and a charged jet of fluid at the tip of the Taylor cone is ejected. During polymer solution is ejected to the collector by whipping process, the solvent is evaporated and stretched reducing in diameter, leaving solid polymer deposited on the collector.

There are several parameters affecting the electrospinning process. These parameters can be separated to 2 main parameter. 1). System parameters such as molecular weight, molecular-weight distribution and architecture of polymer (branched, linear etc.) and properties of solution (viscosity, conductivity and surface tension). 2). Process parameters such as electric potential, flow rate, concentration of solution, distance between the capillary and collector, ambient parameter (temperature, humidity and air velocity in chamber). For example, the solution must have a viscosity high enough and surface tension low enough to prevent the jet collapsing into droplets, yet viscosity not too high that prevent polymer motion, which can be adjusted by concentration of solution [32]. Morphology can be changed by applied voltage. Decreasing applied voltage bead can be more occurred.

Nanofibers prepared by electrospinning were widely utilized in several applications. For example, cosmetic skin mask (skin cleaning, skin healing, skin therapy with medicine, etc.), application in life science (drug delivery carrier, homeostatic devices, wound dressing, etc.), military protective clothing (minimal

impedance to air, aerosol particles, anti-bio-chemical gases, etc.), nano-sensor (thermal sensor, piezoelectric sensor, biochemical sensor, fluorescence optical chemical sensor, etc.), tissue engineering scaffolding (porous membrane for skin, tubular shapes for blood vessels and nerve regenerations, three dimensional scaffolds for bone and cartilage regenerations, etc.), filter media (liquid filtration, gas filtration, particle filtration, etc.) and other industrial applications such as micro/nano electronic devices, electrostatic dissipation, electromagnetic interference shielding, photovoltaic device (nano-solar cell), LCD devices, ultra-lightweight spacecraft materials, higher efficient and functional catalysis, and so on. An application field targeted by patents is mostly medical prosthesis as shown in Fig. 10 [33]. Typically, electrospinning is utilized in a wide range of polymer such as polyvinylalcohol (PVA), polyester, polyvinylpyrrolidone (PVP), polyamide (PA), polyacrylonitrile (PAN) as well as biopolymer like proteins, DNA, polypeptide and others.

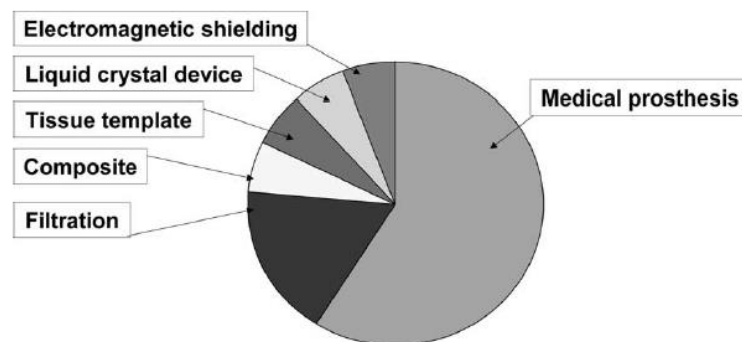


Fig. 10 schematic diagram of application field targeted by patents on electrospun nanofibers [33]

## 2.6 Polyacrylonitrile (PAN)

Polyacrylonitrile is a thermoplastic polymer with chemical formula  $(C_3H_3N)_n$ . Fig. 11 illustrates the chemical structure of PAN repeat unit. PAN was developed for producing of fibers in 1940, after a suitable solvent was discovered by DuPont. The solvents can be dissolved PAN, such as dimethylformamide (DMF), dimethyl sulfoxide (DMSO), dimethylacetamide (DMAc), dimethylsulfone, tetramethylsulfide and aqueous solutions of ethylene carbonate. PAN can be formed as saturated solution with 25% dissolved in DMF at  $50^\circ\text{C}$ , which is highest solubility compared to other solvent. PAN is mostly used as polymer precursor for producing carbon nanofibers (CNFs) due to its high carbon yield (up to 56%). Typically, PAN have an appearance is white powders up to  $250^\circ\text{C}$ , at which point it become darker because of degradation. PAN is high  $T_g$  ( $84\text{-}85^\circ\text{C}$ ), thus it is flexible material at ambient temperature. Having high crystalline melting point ( $317^\circ\text{C}$ ), it is limited to be soluble in solvent and the fibers id superior mechanical properties [34]. In addition PAN is good chemical resistant such as acid, alkaline, alcohols, aliphatic hydrocarbon and aromatic hydrocarbon. Therefore, PAN is often used polymer for producing fibers in many applications [35].

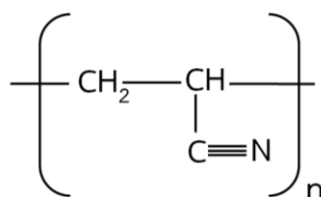


Fig. 11 chemical structure of polyacrylonitrile repeat unit

## 2.7 Literature reviews

The literature reviews is separated in 2 parts; 1) Preparation of photocatalyst nanofibers 2) Photocatalytic degradation of gas-phase VOCs.

### 2.7.1 Preparation of photocatalyst nanofibers

Metal oxide photocatalysts like ZnO or TiO<sub>2</sub> can be synthesized by several methods such as precipitation, sol-gel, chemical vapor deposition (CVD), atomic layer deposition (ALD), hydrothermal, and so on. These methods can synthesize metal oxide nanoparticle to be used as the photocatalyst. However, the photocatalysts in the form of nanoparticles are not practical utilization, which is limited by handling problem. Therefore, many researchers have been attempting to improve the photocatalyst by fabricating the photocatalyst to be in form of nanofibers by electrospinning method so that to overcome handling problem. Moreover, this structure allows high surface-to-volume ratio resulting large exposed area of the photocatalyst. Li et al (2003) [4], Watthanaarun et al (2005) [5], and Tekmen et al (2008) [6] prepared TiO<sub>2</sub> nanofibers by mixing titanium precursor and polyvinylpyrrolidone (PVP) solution, then the solution was loaded into a syringe, after that the solution was electrospun as nanofibers. The as-spun were annealed at high temperature to remove PVP and convert to TiO<sub>2</sub> nanofibers. Park et al (2009) [7] fabricated ZnO nanofibers by mixing Zn precursor and PVP solution, then the solution was drawn as nanofibers with electrospinning technique. The as-spun were

calcined at high temperature, thus PVP was removed and ZnO nanofibers were formed.

However, metal oxide nanofibers were obtained by annealing at high temperature, resulting the nanofibers are brittle, may be crushed into powder. Retaining polymer within the metal oxide nanofibers allowed the nanofibers are more flexible. Many researchers have been attempting fabricate flexible metal oxide nanofibers with various methods. Drew et al (2003) [36] synthesized TiO<sub>2</sub>-coated PAN nanofibers, PAN solution was electrospun into non-woven nanofibers. The nanofibers were then immersed in solution containing titanium precursor to allow TiO<sub>2</sub> coat on the PAN nanofiber surface. Kim et al (2008) [8] prepared TiO<sub>2</sub>/PAN nanofibers by firstly dispersing TiO<sub>2</sub> nanoparticle with polyacrylonitrile (PAN) solution. The suspension was fabricated as composite nanofibers by electrospinning method, which still retained flexibility. Wang et al (2014) [9] fabricated PVA/grapheme oxide (GO)/TiO<sub>2</sub> composite nanofibers by firstly spinning GO/PVA viscous suspension into composite nanofibers. Tetrabutyltitanate (TBT) and ethanol were mixed to allow sol-gel reaction occurred. Then, the composite GO/PVA nanofibers were immersed in the solution, TiO<sub>2</sub> was formed on the surface of nanofibers and PVA/grapheme oxide (GO)/TiO<sub>2</sub> composite nanofibers was obtained.

Although these above methods could synthesize metal oxide-polymer composite nanofibers which still retain flexibility, these metal oxide particles agglomerated, thus the metal oxide particles are not uniform over fibers. Other

method could prepare uniform metal oxide on the polymer nanofibers, for example Sangkhaprom et al (2010) [10] prepared fibrous ZnO by combined electrospinning and solvothermal techniques. Zn precursor and polyvinyl alcohol (PVA) were dissolved in alcohol. The solution was then electrospun into nanofibers, PVA nanofibers containing Zn precursor was obtained. The nanofibers were subsequently subjected to solvothermal with ethanol at moderate temperature (170 – 250°C) for 0-2 hours and therefore ZnO occurred on the PVA fiber with uniform morphology and still possessed flexible property. The same as Su et al (2013) [11] prepared TiO<sub>2</sub>/PAN nanofibers. Titanium precursor and PAN were dissolved in N,N-dimethyl formamide (DMF). The solution was subjected to electrospinning, thereby obtaining Ti-precursor-PAN nanofibers. The obtained nanofibers were subsequently subjected to hydrothermal with deionized water and certain amount of acid and ethanol at 180°C for 10 hours, TiO<sub>2</sub> nanoparticles uniformly decorated on PAN nanofibers was obtained and also still remains flexibility.

Moreover, many researches could synthesized ZnO nanoparticle with various morphology by hydrothermal and solvothermal method such as nanorod, nanowire, nanoflake, and nanosheet. Zinc acetate (Zn(CH<sub>3</sub>COO)<sub>2</sub>), zinc nitrate (Zn(NO<sub>3</sub>)<sub>2</sub>), and zinc chloride (ZnCl<sub>2</sub>) were used as Zn precursors. These precursors were hydrothermalized with various alkali source such as hexamethylenetetramine (HMT) ammonia and sodium hydroxide (NaOH), ZnO nanarods were obtained [12, 13, 37]. Also, ZnO nanorods could be synthesized by solvothermal method. Tonto et al

(2006) [38] prepared ZnO nanorod by solvothermal reaction of zinc acetate in various alcohols.

Growth of ZnO nanorods or nanowires can be arrayed by supplying ZnO seed layer to obtain aligned ZnO nanorods on the seed layer. There are many methods to prepare ZnO seed layer such as atomic layer deposition (ALD), pulse layer deposition (PLD), radio frequency (RF) sputtering, and so on [17-21]. These methods have high cost. Ozturk et al (2012) [20], Thangavel et al (2012) [39], and Schlur et al (2013) [40] prepared ZnO seed layer with a simple method. Zn precursor was coated on the surface of substrate, the coated substrate was then annealed to obtain ZnO layer on the surface of substrate. The ZnO seed layered substrate was immersed in Zn precursor and alkali source solution in DI water to hydrothermal at 90 – 100 °C. Obtaining aligned ZnO nanorods growth on the ZnO seed layer.

Fortunately, if ZnO seeds are deposited on the surface of polymer nanofiber, ZnO nanorods could be decorated on the surface of polymer nanofibers by hydrothermal method. It would increase exposed area and ZnO loading, therefore photocatalytic activity would be increased. Moreover, the fibers would still possess flexibility. From these literature reviews, range of parameter affected on growth of ZnO nanostructures was summarized in table 3. For this study, the studied parameters will be varied by referring from the literature reviews.

Table 3. summary of hydrothermal parameter ranges.

Precursors	Temperatures	Treatment times	Precursor concentration	References
Zinc nitrate, ammonia	100 - 200°C	0.5 – 2 hr	0.5 M	[12]
Zinc nitrate, HMT	60 - 95°C	0.1 – 1 hr	0.01 – 0.1 M	[13]
Zinc chloride, HMT	90°C	3 hr	0.03 M	[15]
Zinc acetate, HMT	140°C	4 hr	0.01	[16]
Zinc nitrate, HMT	90°C	4 hr	0.01	[18]
Zinc acetate, HMT	90°C	3 hr	0.01	[20]
Zinc acetate, NaOH	150°C	4 hr	0.18	[37]
Zinc nitrate, HMT	90°C	10 hr	0.05 M	[39]
Zinc acetate, Ethylenediamine	110°C	2 hr	0.72 M	[40]
Zinc acetate, HMT	95°C	1 hr	0.01 M	[41]
Zinc acetate, HMT	90°C	5 hr	0.02 M	[42]

### 2.7.2 Photocatalytic degradation of gas-phase VOCs

The semiconductor material such as ZnO and TiO<sub>2</sub> was used as photocatalyst for degradation of organic compounds. There are many research have reported photocatalytic degradation of liquid phase organic pollutants such as dyes, and there are a few research have been studying on degradation of gas phase pollutant such as VOCs, sulfur dioxide (SO<sub>2</sub>), nitrogen oxides (NO<sub>x</sub>) and so on. Among gas phase pollutant, VOCs is a mostly attracted gas phase organic pollutant such as benzene, toluene, xylene, acetaldehyde, and so on [2, 43, 44].



The reactor used for photocatalytic process under UV light need to be supplied by UV-lamp. There are many configurations of reactor either batch or continuous flow reactor. A batch reactor was mostly simple to operate in order to study VOC degradation activity. For batch reactor, the photocatalyst was placed in the reactor and UV light was irradiated from outside reactor. For photocatalytic process in degradation of VOCs, water in form of humid gas should be supplied into the reactor so that encourage hydroxyl radical ( $\text{OH}^\bullet$ ) is more generated. In addition, studied parameters such as initial concentration, residence time, and catalyst loading have been studied [45, 46].



## Chapter 3

### Experiment

This chapter aims to describe the experimental methodology for preparation of PAN nanofibers decorated ZnO nanostructures and photocatalytic degradation of toluene. Four parts of this chapter composed of materials, preparation of ZnO nanostructure/PAN nanofibers, characterization, and photocatalytic degradation process.

#### 3.1 Materials

Material used in this work was listed as following;

1. Polyacrylonitrile (PAN), molecular weight  $\sim 150,000$  g/mol, (Sigma-Aldrich)
2. Zinc oxide (ZnO), particle size  $\sim 20$  nm, (Wako Pure Chemical)
3. N,N'-dimethylformamide (DMF),  $(\text{CH}_3)_2\text{NC}(\text{O})\text{H}$ , (Sigma-Aldrich)
4. Zinc acetate,  $(\text{CH}_3\text{COO})_2\text{Zn}\cdot 2\text{H}_2\text{O}$ , (Ajax Finechem)
5. Hexamethylenetetramine (HMT),  $\text{C}_6\text{H}_{12}\text{N}_4$ , (HIMEDIA)
6. Deionized water
7. Toluene,  $\text{C}_7\text{H}_8$ , (Fisher chemical)

#### 3.2 Preparation of ZnO nanostructure/PAN nanofibers

### 3.2.1 Preparation of suspension of ZnO nanoparticles in PAN solution

ZnO powders suspended in 8 %wt of PAN solution in DMF with ZnO/PAN ratio of 1:1 will be prepared by firstly adding ZnO powders in 10 ml of DMF and dispersing by stirring for 15 min and ultrasonication for 15 min. Subsequently, PAN will be adding into the suspension and stirring for 2 hours at 60°C. Before electrospinning, the mixture will be ultrasonicated for 20 min.

### 3.2.2 Preparation of composite ZnO/PAN nanofibers

The ZnO/PAN mixture will be poured into 10 ml plastic syringe with a needle. The syringe containing ZnO/PAN mixture will be installed to syringe pump. The composite ZnO/PAN nanofibers will be prepared by electrospinning apparatus as shown in Fig. 12. The electrospinning apparatus consists of a high voltage power supply (GAMMA VOLTAGE RESEARCH, ORMOND BEACH, FL 32174), the syringe with needle, and a collector which aluminium foil used as. The power supply will generate the different electric potential voltage between the needle and collector. Therefore, the ZnO/PAN mixture will be drawn as fibers and deposited on the collector, obtaining the composite ZnO/PAN nanofibers. For conditions of electrospinning process, will be conducted at 17 kV supplied voltage, 20 cm of distance between the needle and collector, 0.8 ml/hr flow rate of the syringe pump.

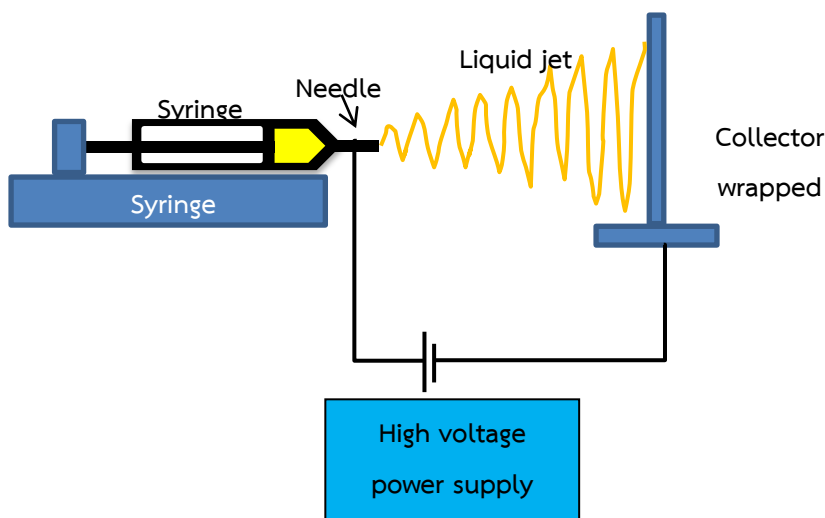


Fig. 12 schematic of electrospinning process

### 3.2.3 Growth of ZnO nanostructures on the composite ZnO/PAN nanofibers

The fibers deposited on collector will be cut into a dimension of 10x12 cm and peeled out from aluminum foil. Zinc precursor is provided by zinc while alkali source is provided by hexamethylenetetramine (HMT). Zinc acetate and HMT will be simultaneously dissolved in 40 ml deionized water, which concentration of zinc acetate will be varied by 0.03, 0.06, and 0.12 M, meanwhile concentration of HMT will be varied by adjusting zinc acetate/HMT ratio with 1:2, 1:1, and 2:1. The 40 ml of precursor solution will be poured into a reactor. The reactor used is a Teflon line sealed stainless steel autoclave as shown in Fig. 13.



Fig. 13 Autoclave reactor

To growth of ZnO nanostructure on PAN nanofiber surfaces, the reactor will be placed in an oven and the hydrothermal process will be conducted at temperature varied by 100, 140, and 180°C for 1, 2, and 4 hours. After that the autoclave will be took out and cooled down in cool water bath so that reaction is stopped. The hydrothermal fibers will be removed from autoclave and subsequently dried in oven. The ZnO nanostructure/PAN nanofibers will be obtained. The conditions which will be studied in this work were shown in Fig. 14.

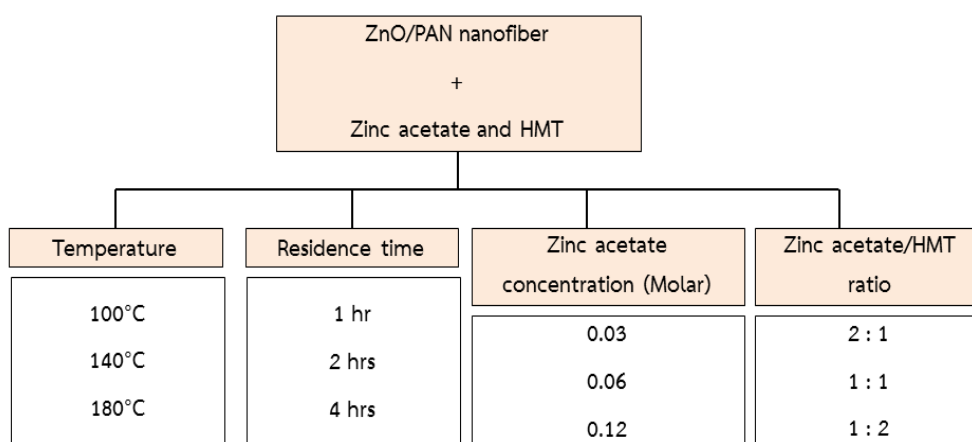


Fig. 14 Condition of hydrothermal experiment diagram

### 3.3 Characterization

#### 3.3.1 Scanning electron microscopy (SEM)

The morphology of ZnO nanostructure/PAN nanofibers prepared will be observed by Jeol JSM-6400 scanning electron microscopy (SEM) with 5.0 kV at Scientific and Technological Research Equipment Centre Foundation (STREC), Chulalongkorn University. To specimens be electrical conducting, the specimens need to be coated by Au before characterization.

#### 3.3.2 Atomic Absorption Spectroscopy (AAS)

Residual zinc acetate in the autoclave was determined in form of zinc content by using Atomic Absorption Spectroscopy (AAS) at Scientific and Technological Research Equipment Centre Foundation (STREC), Chulalongkorn University. The samples will be participated in order to separate residual ZnO particle before determination.

#### 3.3.3 The Brunauer-Emmett-Teller (BET)

The surface areas of ZnO nanostructure/PAN nanofibers prepared will be determined by the Brunauer-Emmett-Teller (Belsorp II) at Center of Excellence in Particle Technology, Chulalongkorn University.

#### 3.3.4 Universal Testing Machine

Flexibility of ZnO/PAN nanofibers prepared will be determined in form of tensile strength by Universal Testing Machine. Comparison of each sample will be shown as stress-strain curve.

### 3.4 Photocatalytic degradation process

Photocatalytic degradation process will be operated under batch photoreactor. The UV lamp was placed outside the transparent batch reactor. The UV light could be transmitted into inside reactor. The photograph of photoreactor was shown as Fig. 15. Volume of reactor is 9 ml. The ZnO nanostructure/PAN nanofibers are around 0.1 g depend on hydrothermal conditions was placed inside the reactor. The cap of the reactor is a septum. It can be fed or remove gas into/from the reactor.

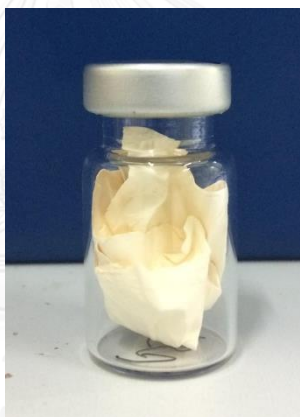


Fig. 15 photograph of photoreactor

Toluene was chosen as model VOCs. The toluene vapor will be generated by bubbling process using air as bubbling gas, which the concentration of toluene will be controlled by adjusting air flow rate. The gaseous toluene in air was filled in gas bag. Designed amount of toluene gas was fed into the reactor to obtain proper concentration of toluene in the reactor. This work prepared toluene concentration of

430 ppm, which is proper for photocatalytic reaction. Humidity is 50%RH in order to encourage more  $\text{OH}^\bullet$  generation.

The reactor containing ZnO/PAN nanofibers and toluene gas was irradiated by UV light. The sample was determined toluene concentration at 1, 2, 4, and 6 hrs by FID gas chromatography (FID-GC) in the model of SHIMADZU GC-148. Performance of toluene removal can be represented by conversion or reaction rate constant.





## Chapter IV

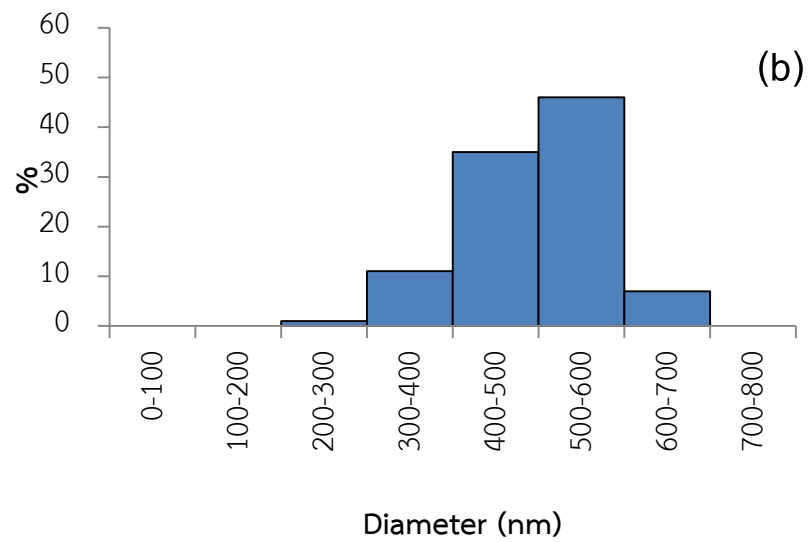
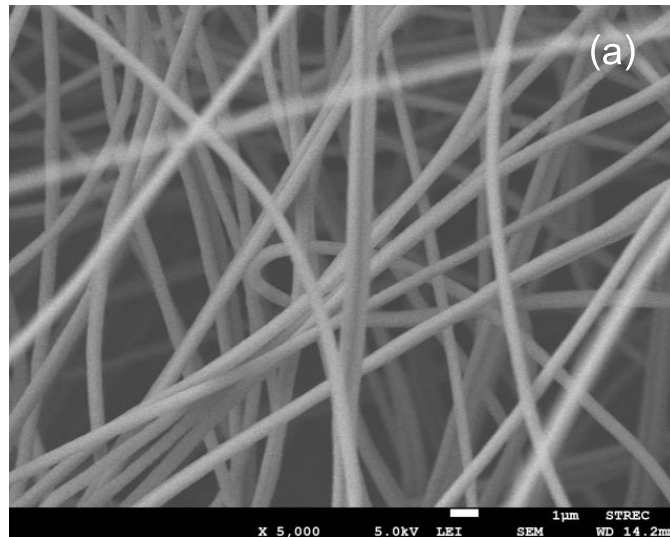
### Results and Discussion

This chapter describes all experimental and analytical results. It is composed of 1). Experiments on fabrication of flexible ZnO/PAN nanofibers take into account effects of zinc acetate, temperature, treatment time, and zinc acetate:HMT ratio, 2). Experiments on photocatalytic degradation of VOC and, 3). analysis of mechanical properties of prepared nanofibers.

#### 4.1 Fabrication of flexible ZnO/PAN nanofibers

ZnO seeds were suspended in PAN solution and then the suspension was subjected to electrospinning process. The added ZnO seeds would act as nucleation sites for ZnO nanorod growth. Fig. 16a is a SEM image of PAN nanofibers. It was found that the surfaces of fibers were smooth and the average fiber diameter was 497 nm based on statistical analysis shown in Fig. 16b. Fig. 16c shows morphology of ZnO seeds/PAN nanofibers under SEM observation. It was found that the surface of fibers possess roughness higher than that of the PAN nanofibers because there are many ZnO seeds existing on the fiber surface. ZnO seeds were uniformly dispersed within PAN nanofibers. Such morphology should be favorable for ZnO nanorod growth. The ZnO seeds/PAN nanofibers possesses average diameter of 317 nm confirmed by

statistical analysis shown in Fig. 16d. It was found that the average diameter of ZnO seeds/PAN nanofibers is lower than that of PAN nanofibers.



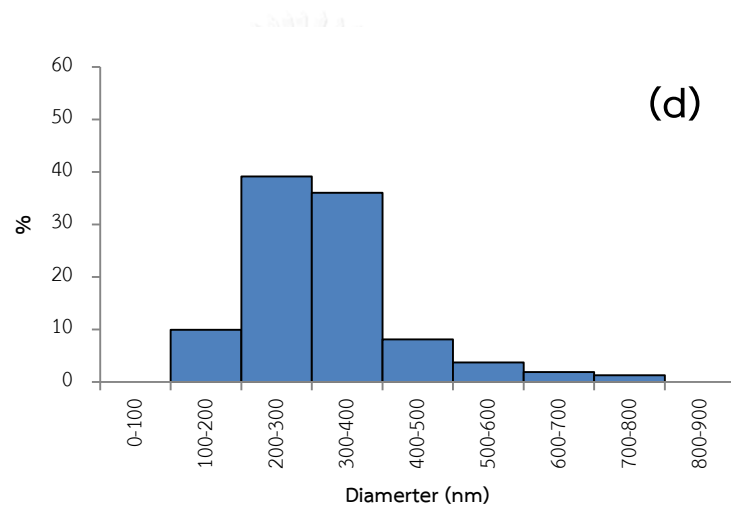
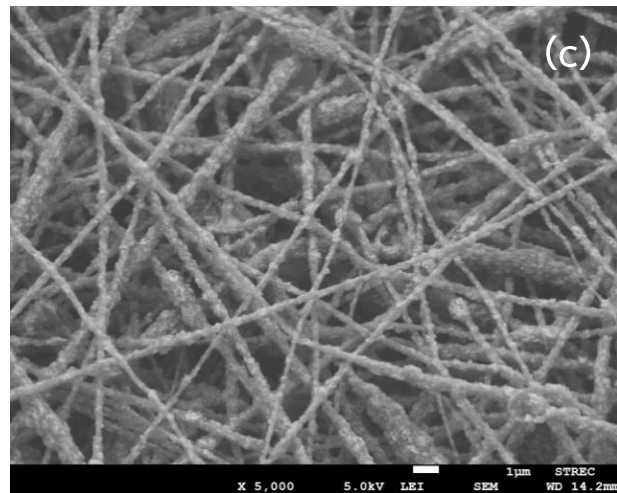


Fig. 16 SEM images (a, c) and diameter size distribution (b, d) of PAN and ZnO seeds/PAN nanofibers.

Hydrothermal treatment was utilized for ZnO nanorod growth on the PAN nanofibers using zinc acetate and HMT as reactants. For this process, 4 effects was studied

#### 4.1.1 Effect of zinc acetate concentration

Concentration of zinc acetate was varied by 0.03, 0.06, and 0.12 molar with 1:1 zinc acetate:HMT ratio. The hydrothermal process was operated at 140°C for 2 hrs. Fig.17 shows SEM images of hydrothermalized ZnO/PAN nanofibers from various zinc acetate concentration. It was found that ZnO nanorods could grow on the surface of PAN nanofibers. Therefore, this ZnO structure is proper for photocatalytic degradation.

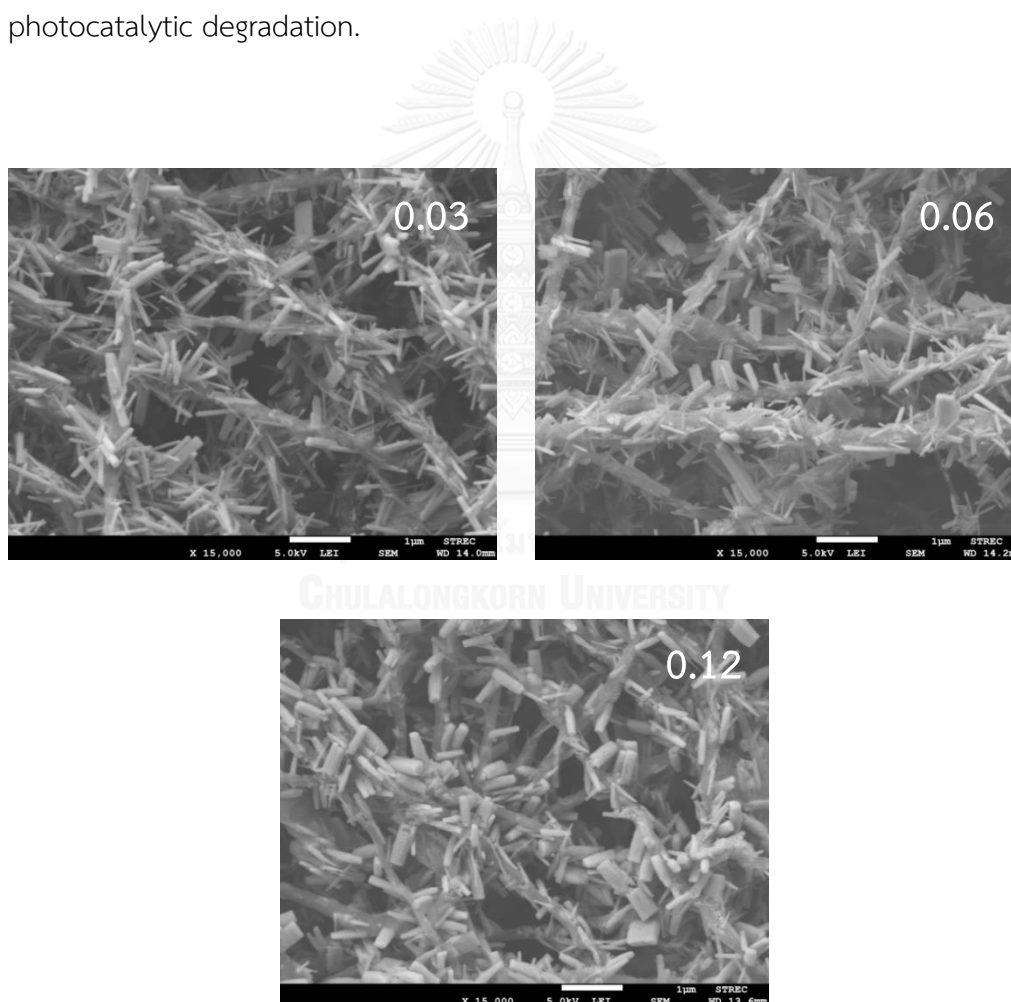
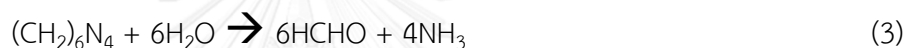
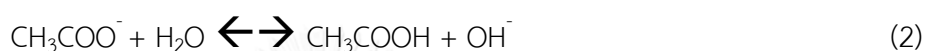


Fig.17 SEM images of hydrothermalized ZnO/PAN nanofibers from various zinc acetate concentration (M)

ZnO nanorods growth could be occurred by hydrothermal process of zinc acetate and HMT by supplying ZnO seeds during the process. Zinc acetate could provide  $\text{Zn}^{2+}$  and HMT could provide  $\text{OH}^-$  therefore ZnO could be formed as follows [20, 39, 47-51]



ZnO crystal has distinct planes which are polar plane (0001) and non-polar plane (0110). The polar plane has surface energy is higher than non-polar plane. Therefore, the crystal growth prefers to grow at the (0001) plane in c-axis direction, resulting in the crystal has a shape of nanorod [52].

ZnO nanorods growing on the surface of PAN nanofibers from different zinc acetate concentration demonstrate different dimensions such as diameter and length. Fig. 18 shows average diameter and length of ZnO nanorods from various zinc acetate concentration. It was found that ZnO nanorods prepared from 0.03, 0.06, and 0.12 molar possess average diameter of 60, 76, and 131 nm respectively. The length of ZnO nanorods is 499, 397, and 405 when zinc acetate concentration was varied 0.03, 0.06, and 0.12 molar respectively. At low concentration, there are low  $\text{Zn}^{2+}$  and  $\text{OH}^-$ , resulting in less collision rate of growth. There is enough time to grow along (0001) direction. On the other hand, at high concentration, there is lots of  $\text{Zn}^{2+}$  and  $\text{OH}^-$ , resulting in higher collision rate of growth. Therefore, there is not enough time to grow along (0001) direction. It needs to grow (0110) direction, resulting in larger diameter of ZnO nanorods [53].

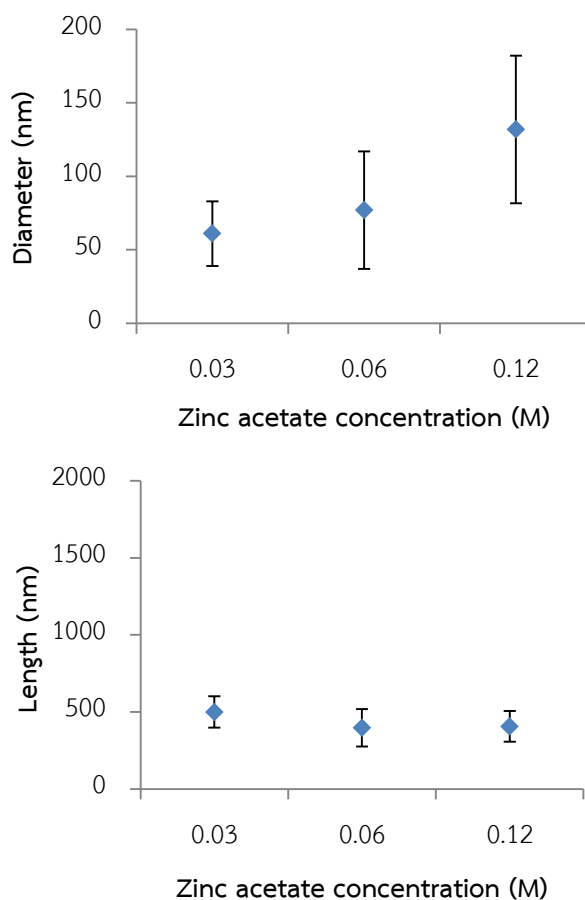


Fig. 18 diameter and length of ZnO nanorods prepared by various zinc acetate concentration

ZnO loading is an important factor for photocatalytic reaction. This ZnO/PAN nanofiber preparation method could load many of ZnO on the fibers. The zinc acetate concentration was expected that is important parameter to ZnO loading. Fig. 19 shows percentage of increased weight of ZnO/PAN nanofibers after hydrothermal process. The increased weight can be calculated by equation (7). The increased weight could represent ZnO loading.

$$\text{Increased weight} = \frac{\text{weight after} - \text{weight before}}{\text{weight before}} \times 100 \quad (7)$$

It was found that when zinc acetate concentration was increased from 0.03 molar to 0.12 molar, increased weight was increased from 13% to 48%. Therefore, higher zinc acetate concentration could be obtained higher ZnO loading. Based on higher zinc acetate concentration, there are higher amount of reactant for ZnO nanorod growth and also higher concentration encourage higher reaction rate as rate law.

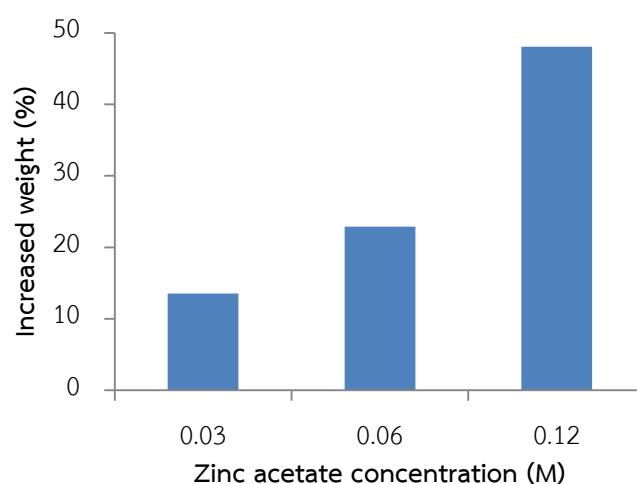


Fig. 19 percent of increased weight of fibers after hydrothermal process of various zinc acetate concentration

#### 4.1.2 Effect of temperature

Temperature was expected that could influence ZnO nanorod growth. The temperature was varied by 100, 140, and 180°C for 2 hrs, zinc acetate concentration was prepared for 0.03 molar with 1:1 zinc acetate:HMT ratio. Fig. 20 shows SEM images of ZnO/PAN nanofibers prepared at various temperatures. It was found that the ZnO/PAN nanofibers obtained from hydrothermal treatment at various temperatures have different dimension. Fig. 21 demonstrates diameter and



length of ZnO nanorods at various hydrothermal temperatures. When the temperature was increased from 100°C to 140°C, average diameter was increased from 40 nm to 60 nm and length was increased from 353 nm to 499 nm. When temperature was increased from 140°C to 180°C, average diameter was not varied. While average length increased to 1,184 nm.

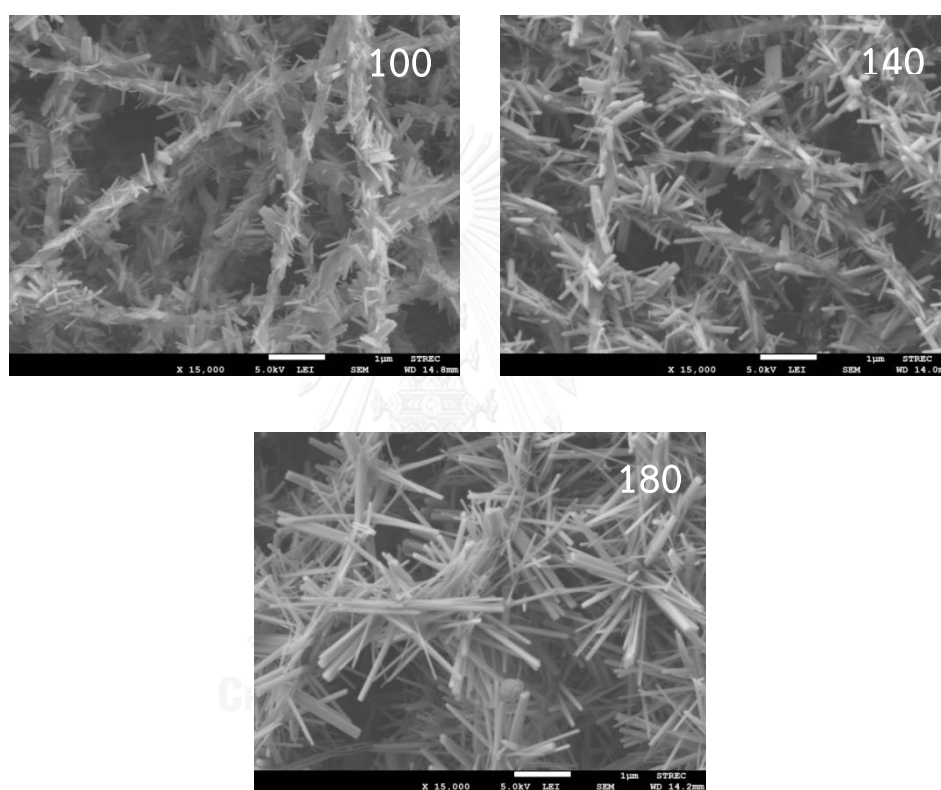


Fig. 20 SEM image of ZnO/PAN nanofibers prepared by various temperatures (°C).

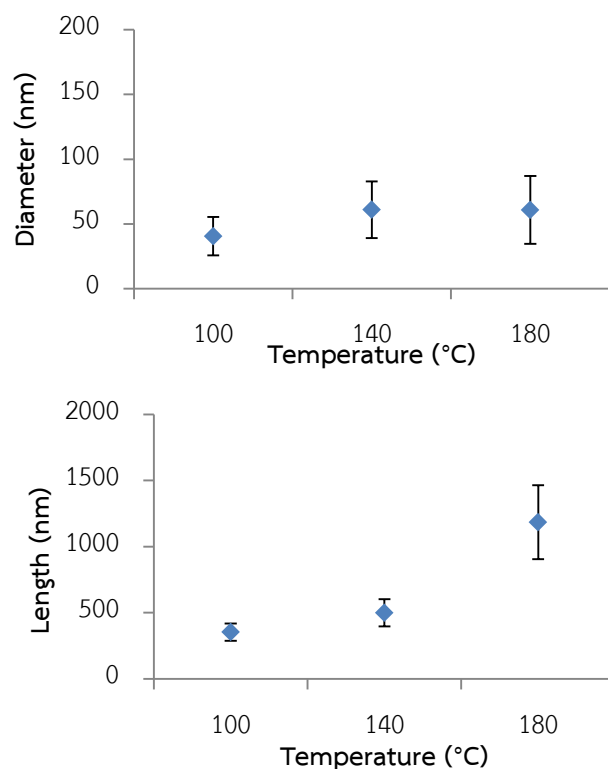


Fig. 21 average diameter and length of ZnO nanorods prepared by various temperatures

These average diameter and length is corresponding to ZnO loading in the fibers which was exhibited in form of percentage of increased weight which could be calculated by equation (7). Fig. 22 demonstrates percentage of increased weight after hydrothermal treatment at various temperatures. When hydrothermal temperature was increased from 100°C to 140°C and 180°C, the increased weight increased from 10 to 13 and 18% respectively. It could be ascribed that increasing temperature could increase growth rate. The growth rate depended on synthesized temperature which could be expressed by Arrhenius equation as following equation (8).

$$r = A \exp(-Ea/RT) \quad (8)$$

Where  $r$  is the growth rate,  $E_a$  is activation energy,  $R$  is gas constant, and  $T$  is the temperature. The  $E_a$  value was found by Zhou et al.[54] and Cheng et al.[55] are 80.52 and 35  $\text{kJ/mol}^{-1}$  respectively. Therefore, variation of temperature could influence growth rate. As the Arrhenius equation, it could be expected that increase temperature contribute to increase growth rate which is corresponding to the results of experiment.

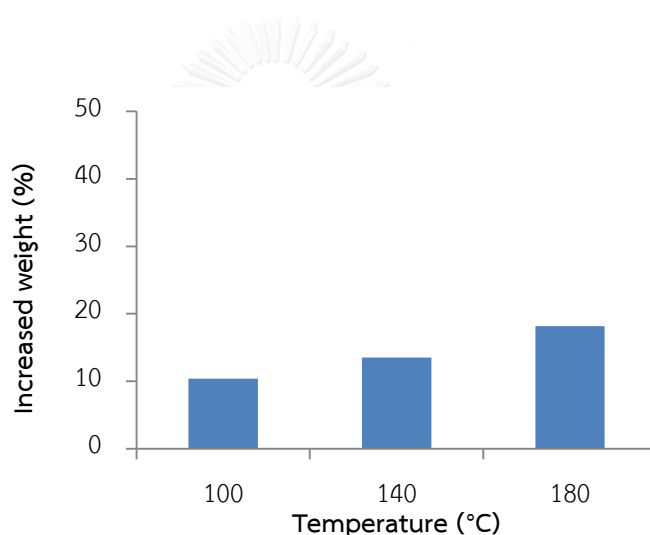


Fig. 22 percentage of increased weight of fibers after hydrothermal treatment at various temperatures.

In addition, amounts of zinc acetate remaining in the autoclave reactor after hydrothermal treatment were also determined. The remaining zinc acetate was represented by amount of Zn content in the solution. Table 4 shows Zn content remaining in the autoclave after hydrothermal treatment by various treatment temperatures. Zn contents remaining in the solution are 744, 234, and 26  $\text{mg/L}$  after hydrothermal treatment at 100, 140 and 180°C respectively. While Zn

content before hydrothermal treatment is 1,995 mg/L. It was found that hydrothermal treatment at 180°C contributes to highest rapidly decreasing of Zn content. At 180°C remaining Zn content is almost completely consumed within 2 hrs. Due to higher temperature encourages enhancing reaction rate as could be described by Arrhenius equation as well. The consumed zinc acetate was expected that was consumed for ZnO nanorod growth. This is also supported that at high treatment temperature obtains higher ZnO loading. Therefore, preparation of ZnO/PAN nanofibers by hydrothermal treatment at higher temperature could be obtained higher ZnO loading.

Table 4. residual Zn contents in the autoclave after hydrothermal treatment at various temperatures

Treatment temperature (°C)	Residual Zn content (mg/L)
100	744
140	234
180	26

#### 4.1.3 Effect of treatment time

The treatment times were expected that could affect to growth of ZnO nanorods and ZnO loading. The experiments were conducted by varying the treatment times for 1, 2, and 4 hrs at 140°C and 0.03 molar of zinc acetate concentration. Fig. 23 shows SEM images of ZnO/PAN nanofibers prepared with

various treatment times. All of that treatment time could be obtained ZnO nanorods equally growing on the surface of PAN nanofibers as Fig. 24 demonstrate the diameter and length of ZnO nanorods obtained from various treatment times. The diameters of ZnO nanorods for various treatment times were not varied. While the length of ZnO nanorods gradually increase, when treatment time was increased. It was found that increase treatment times could just gradually increase ZnO nanorods growth rate.

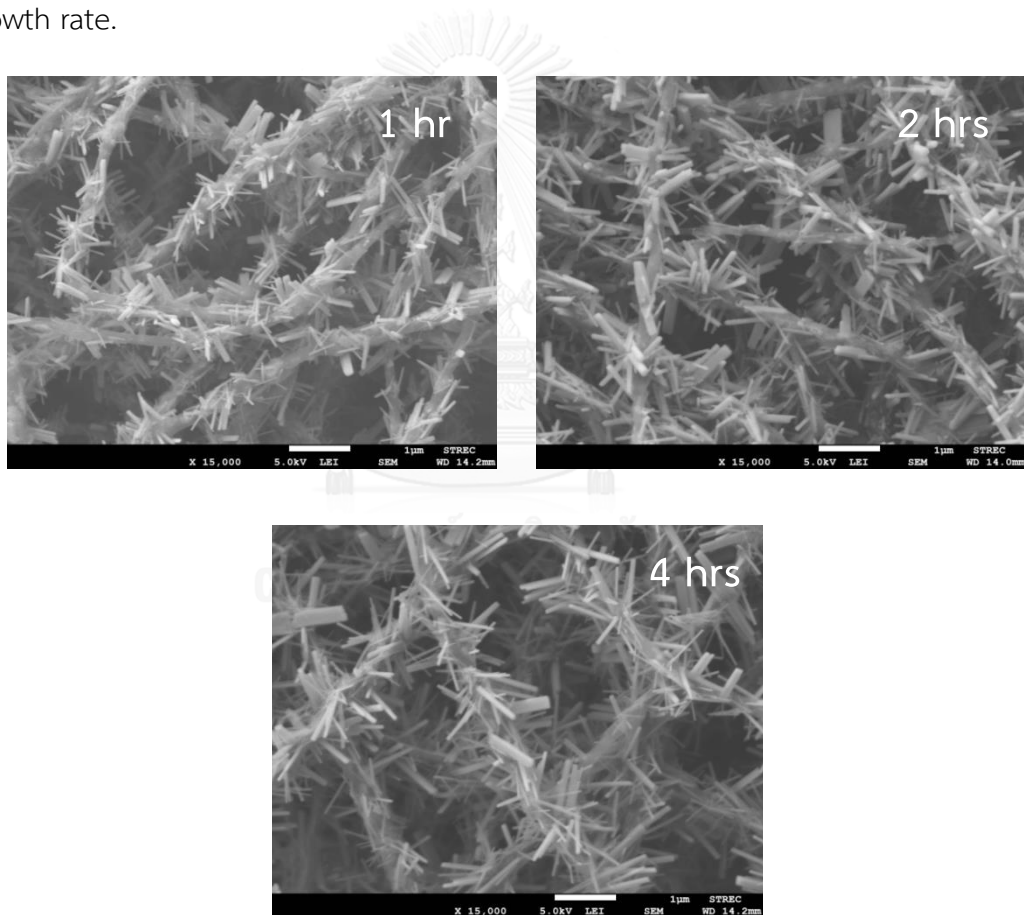


Fig. 23 SEM images of ZnO/PAN nanofibers prepared by various treatment times

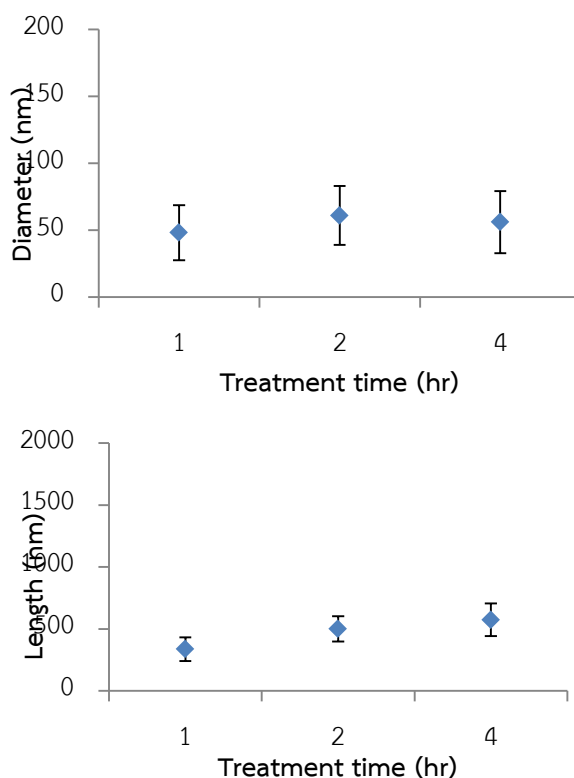


Fig. 24 average diameters and lengths of ZnO/PAN nanofibers prepared by various treatment times.

Regarding to low ZnO nanorod growth rates, ZnO loading in the fibers were not significantly increased as showed in Fig. 25. Fig. 25 demonstrates ZnO loading in form of increased weight of fibers which is calculated by equation (7). All of treatment times could equally load ZnO nanorods in the fibers around 13%. Due to treatment time after 1 hr, zinc acetate was greatly consumed therefore concentration of zinc acetate in the reactor lightly remain as Table 5 showed remaining Zn content in the reactor after hydrothermal treatment for various treatment times. Lower concentration of reactant result in lower reaction rate therefore this is because ZnO loading is not varied.

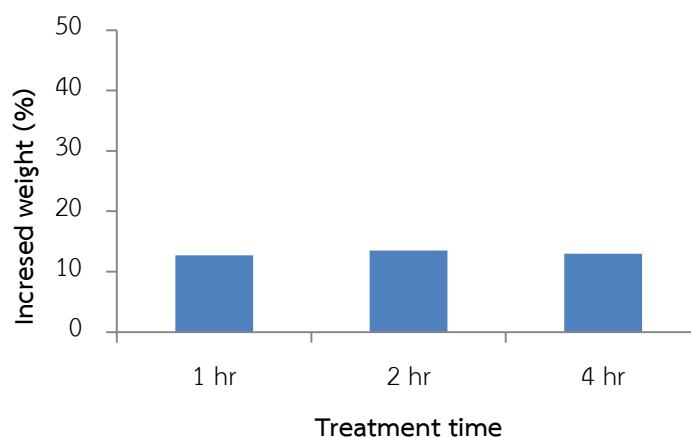


Fig. 25 percent of increased weight of fibers after hydrothermal treatment for various treatment times.

Table 5. Residual Zn contents in the autoclave after hydrothermal treatment for various treatment times

Treatment time (hrs)	Residual Zn content (mg/L)
0	1995
1	273
2	234
4	122

These ZnO/PAN nanofibers prepared by various conditions are different in morphology, ZnO loading. In addition, surface area is an important parameter for VOCs removal, various nanofibers possess specific surface area as shows in Table 6 It was found that PAN nanofibers have a specific surface area of 10 m<sup>2</sup>/g. Once ZnO seeds were subjected to the PAN nanofibers, the surface area was increased to 19 m<sup>2</sup>/g. After hydrothermal treatment, ZnO nanorods grow on the surface of PAN nanofibers, the specific surface area was gradually increased to 20 –

24  $\text{m}^2/\text{g}$ . However, the surface areas of ZnO/PAN nanofibers prepared by various hydrothermal conditions were not significantly different.

In addition, average diameter of various nanofibers was determined as shown in Fig. 26. It was found that only PAN nanofibers possess average diameter of 498 nm. When ZnO seeds were added to the PAN solution and was subjected to electrospinning process, average diameter of fibers was decreased to 414 nm. Therefore, this is because specific surface area was increased after ZnO seeds were added to the fibers. It could be confirmed that decrease of diameter of fibers contribute to increase specific surface area as could be seen that PAN and ZnO/PAN nanofibers subjected to hydrothermal treatment possess lower fiber diameter and contribute to increase specific surface area from 10 to 15  $\text{m}^2/\text{g}$  and 19 to 27  $\text{m}^2/\text{g}$  respectively.

Table 6. specific surface areas of various nanofibers.

Types of fibers	Specific surface area ( $\text{m}^2/\text{g}$ )
PAN	10
ZnO/PAN	19
Hydrothermalized PAN	15
Hydrothermalized ZnO/PAN	27
0.03 M	23
0.06 M	23
0.12 M	20
100°C	21
140°C	23
180°C	22



1 hr	22
2 hrs	23
4 hrs	24

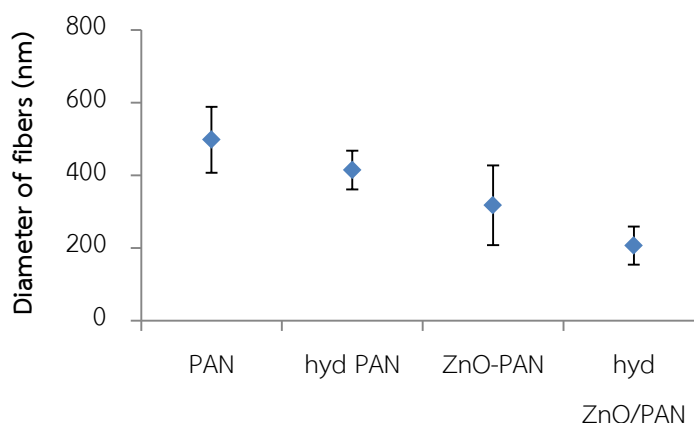


Fig. 26 average diameter of various fibers

#### 4.1.4 Effect of zinc acetate:HMT ratio

Zinc acetate could provide  $\text{Zn}^{2+}$  and HMT could provide  $\text{OH}^-$  which  $\text{Zn}^{2+}$  and  $\text{OH}^-$  could form ZnO. According to equation (1)-(6) mole ratio of  $\text{Zn}^{2+}$  and  $\text{OH}^-$  is 1:2. However, mole ratio of zinc acetate and HMT should be studied because of limiting reagent subject. Zinc acetate:HMT mole ratio were varied by 2:1, 1:1, and 1:2. Fig. 27 show SEM images of ZnO/PAN nanofibers prepared by various zinc acetate:HMT ratio at 140°C for 2 hrs and 0.03 M of zinc acetate concentration. It was found that ZnO/PAN nanofibers prepared by 2:1 zinc acetate:HMT ratio have terrible ZnO growth as low aspect ratio of ZnO nanoparticle on the surface of PAN nanofibers because there was not enough  $\text{OH}^-$  for supply to  $\text{Zn}^{2+}$ . Therefore, slough of excess zinc acetate residue in the fibers. For 1:1 zinc acetate:HMT ratio, it was

found that ZnO nanorods could well grow and there are not any residual zinc acetate in the fibers. Therefore, this ratio may be proper for preparation of ZnO/PAN nanofibers. For 1:2 zinc acetate:HMT ratio, the ZnO nanorods could also well grow but there are slough of excess HMT residue in the fibers because there was too much HMT. Therefore, this ratio is not proper because of excess HMT.

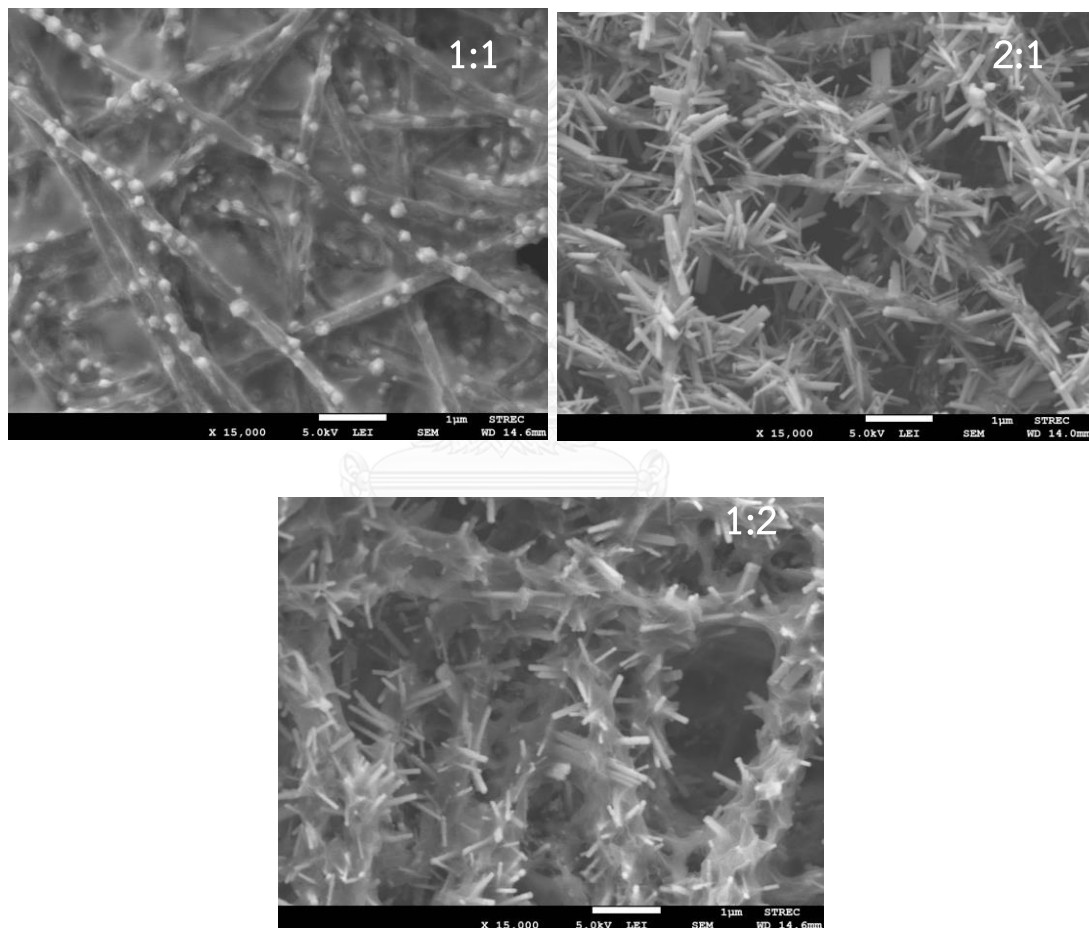


Fig. 27 SEM images of ZnO/PAN nanofibers prepared by various zinc acetate:HMT ratio.

#### 4.2 Mechanical properties of ZnO/PAN nanofibers

The ZnO/PAN nanofibers were anticipated to utilize in air treatment process. For favorable usability, the fibers need for flexibility. Therefore, this work attempted to fabricate flexible ZnO/PAN nanofibers. At least the fibers should be bended without fracture. Fig. 28 shows photograph of bending of ZnO/PAN nanofibers after hydrothermal treatment. It was seen that the ZnO/PAN nanofibers could be bended without fracture. Therefore, the ZnO/PAN nanofibers prepared by this method possess flexibility that is proper for using in air treatment process.



Fig. 28 photograph of bending of ZnO/PAN nanofibers after hydrothermal treatment.

However, scientific mechanical values should be also showed. The ZnO/PAN nanofibers were tested by tensile test. Stress-strain curve was demonstrated as showed in Fig. 29 and also Fig. 30 demonstrates modulus. The modulus could be obtained from slope of stress-strain curve. It was found that pure PAN nanofibers have low strength and modulus which is observed by height of peak and less steep

slope, which have average strength and modulus are 0.36 MPa and 1.78 respectively. However, elongation at break is high. Due to the as-spun nanofibers is spongy. When it was pulled, the fibers would be oriented in prior to it were elongated. As a result, the modulus is low. When the ZnO nanoparticles were added into the PAN nanofibers as composite nanofibers, both strength and modulus significantly decreased to 0.10 MPa and 0.15 respectively. Due to adding ZnO nanoparticles results in multiphase material. If ZnO nanoparticles were added with suitable amount, mechanical properties would be worse. In this case the ZnO nanoparticles were added too much in order to supply many nucleation sites resulting in poor mechanical properties. However, both strength and modulus increase after hydrothermal treatment. Average strength increase to 0.58 MPa after hydrothermal treatment at 180°C. Also, average modulus increase to 6.0 MPa after hydrothermal treatment at 180°C. Due to the fiber mats undergone hydrothermal treatment were soaked by the solution and then dried for water removal, resulting in shrinkage of fiber mats as thickness of fiber mats decrease 50%. When the fiber mats were pulled, the fibers would be elongated without fiber orientation. Therefore, modulus of ZnO/PAN nanofibers after hydrothermal treatment is higher than that before.

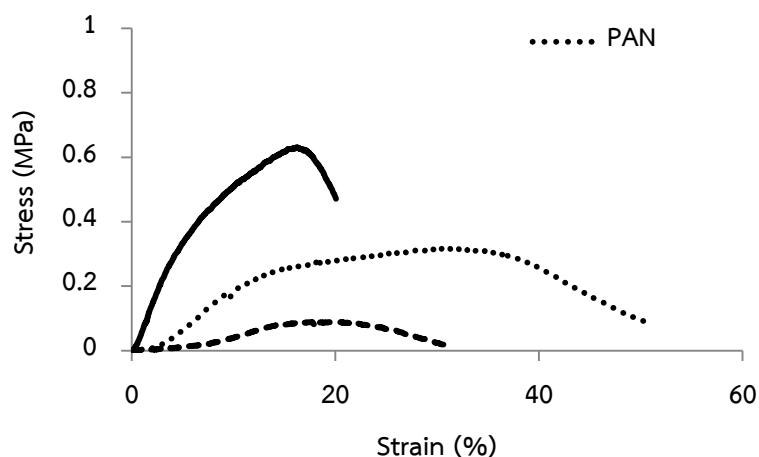


Fig. 29 stress-strain curve of various ZnO/PAN nanofibers

It was also found that increase hydrothermal temperature could enhance modulus. It was found that ZnO/PAN nanofibers after hydrothermal treatment at 100, 140, and 180°C have tensile modulus of 3, 5, and 6 MPa respectively. It is well known that increase treatment temperature would contribute to higher crystallinity. When polymer possesses high crystallinity, the modulus should be increased. Ravandi et.al [56] also reported that PAN nanofibers treated at higher temperature is more crystallinity, resulting in higher modulus.

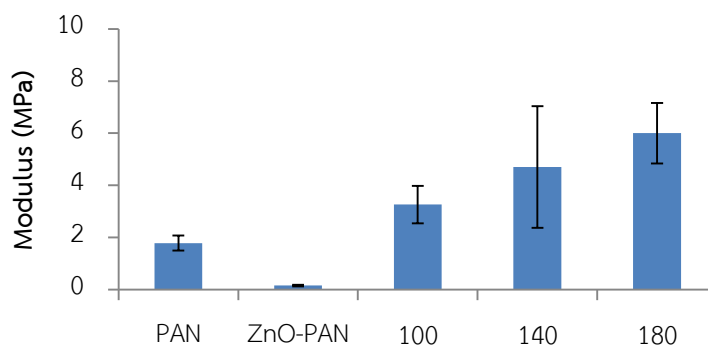
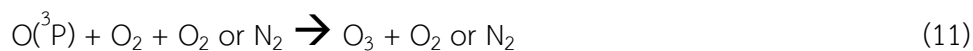
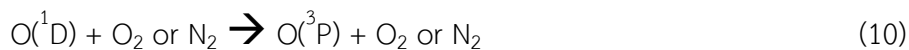


Fig. 30 modulus of ZnO/PAN nanofibers before and after hydrothermal treatment at various temperatures.

### 4.3 Photocatalytic VOC degradation

The ZnO/PAN nanofibers prepared by various conditions have different properties. Therefore, these ZnO/PAN nanofibers would be examined performance for photocatalytic VOC degradation. Toluene was chosen as delegate of gaseous VOCs. The photocatalytic VOC degradations were operated in batch reactor. The concentrations of toluene were detected each reaction times. The objective of this work is to study effects from variables of hydrothermal treatment which consist concentration of zinc acetate, temperature, and treatment time on photocatalytic activity of the prepared ZnO/PAN nanofibers.

Fig. 31 shows performance of toluene removal by each type of nanofibers.  $C/C_0$  was plotted against reaction times. It was seen that at initial time ( $t=0$ )  $C/C_0$  is 1. When the reactions proceed,  $C/C_0$  decrease due to the toluene was removed by adsorption and photocatalytic reaction. It was found that when gaseous toluene was exposed by only UV light in absence of any nanofibers, toluene could be photodegraded by photochemical oxidation because of UV light. Toluene concentration could be removed so that remains 43% within 2 hrs. In dry air, reactive oxygen species such as  $O_3$  and  $O(^1D)$  could be form via gas-phase reaction in equation (9)-(12) [57]. Moreover, in humid air, hydroxyl radical ( $OH^\bullet$ ) could be also formed via equation (13)-(14) [57]. Therefore, it contributes to photochemical oxidation of organic compounds due to the strong formed oxidative species.



In presence of ZnO and UV, ZnO/PAN nanofibers were loaded to the process. Toluene could be removed faster as toluene concentration remains 22% and 14% within 2 and 4 hrs respectively. ZnO could behave as photocatalyst that accelerate generation on hydroxyl radical ( $\text{OH}\cdot$ ). When ZnO was irradiated by UV light, hole ( $\text{h}^+$ ) and electron ( $\text{e}^-$ ) could be generated as equation (15) [58]. Hole ( $\text{h}^+$ ) is oxidizing agent and could generate more hydroxyl radical as oxidative reaction expressed by equation (16) [58] so that toluene was faster degraded by photocatalytic reaction.



When ZnO/PAN nanofibers were subjected to hydrothermal treatment, ZnO was more loaded as ZnO nanorods on the surface of PAN nanofibers for 13%. It was found that toluene concentration remains 4% within 2 hrs and toluene could be completely degraded within 4 hrs. ZnO/PAN nanofibers undergoing hydrothermal treatment could enhance performance of photocatalytic toluene removal because of loaded ZnO nanorods. However, to confirm effect of ZnO loading on performance of photocatalytic toluene removal, ZnO nanoparticle was added into ZnO/PAN nanofibers with equal mass of ZnO grown by hydrothermal treatment. It was found that performance of toluene removal is similar to ZnO/PAN nanofibers undergoing hydrothermal treatment. Therefore, it could confirm that ZnO/PAN nanofibers undergoing hydrothermal treatment could enhance performance of photocatalytic toluene removal because of increased ZnO loading.

Unless photocatalytic reaction, adsorption might occur in the process and contribute to remove gaseous toluene. Therefore, effect of adsorption was studied in absence of light in order to inhibit photocatalytic reaction. Toluene concentration remains 39% within 2 hrs due to adsorption by PAN nanofibers. The concentration of toluene could remain 18% within 2 hrs by adsorption using ZnO/PAN nanofibers. It was found that ZnO/PAN nanofibers have adsorption performance is higher than PAN nanofibers due to ZnO/PAN nanofibers have specific surface area is higher than PAN nanofibers as showed in Table 6.



Meanwhile, ZnO/PAN nanofibers undergoing hydrothermal treatment could adsorb gaseous toluene so that toluene concentration remains 24%. When UV light was irradiated to the process, toluene was removed so that remains 4% within 2 hrs and completely removed within 4 hrs. Therefore, it could be confirmed that photocatalytic reaction occurred and contribute to higher performance in toluene removal process. Moreover, it could be seen that increase ZnO loading by hydrothermal treatment could enhance performance of photocatalytic degradation of toluene. Loading ZnO into fibers by various hydrothermal treatment conditions might affect to performance of photocatalytic degradation of toluene. Therefore, effects of hydrothermal treatment on performance of toluene removal should be also studied.

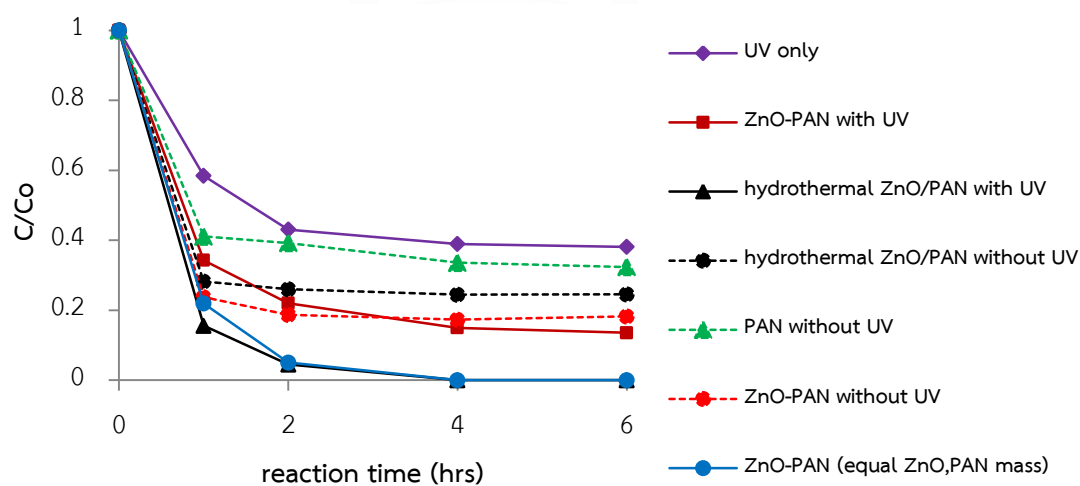


Fig. 31 Toluene removal by various photocatalysts.

For study performance of photocatalytic reaction without adsorption, degradation process was conducted after adsorption equilibrium. Therefore toluene removal was affected by photocatalytic reaction only. Fig. 32 shows photocatalytic degradation of toluene in batch reactor by ZnO/PAN nanofibers before and after hydrothermal treatment. It was found that ZnO/PAN nanofibers after hydrothermal treatment have performance that is better than that of before hydrothermal one. Mole balance was defined as equation (17). The reaction was considered as first order reaction [59, 60]. Rate law was shown in equation (18). It could be derived as equation (19-20). Fig. 33 plots  $\ln \frac{C_{A0}}{C_A}$  against reaction time. The reaction rate constant (k) could be expressed by slope. The reaction rate constant (k) of toluene degradation by ZnO/PAN nanofibers before and after hydrothermal treatment are 0.39 and 1.50 hr<sup>-1</sup>.

$$\frac{dC_A}{dt} = -kC_A \quad (17)$$

$$r = kC_A \quad (18)$$

$$\ln C_A = -kt + C_{A0} \quad (19)$$

$$\ln \frac{C_{A0}}{C_A} = kt \quad (20)$$

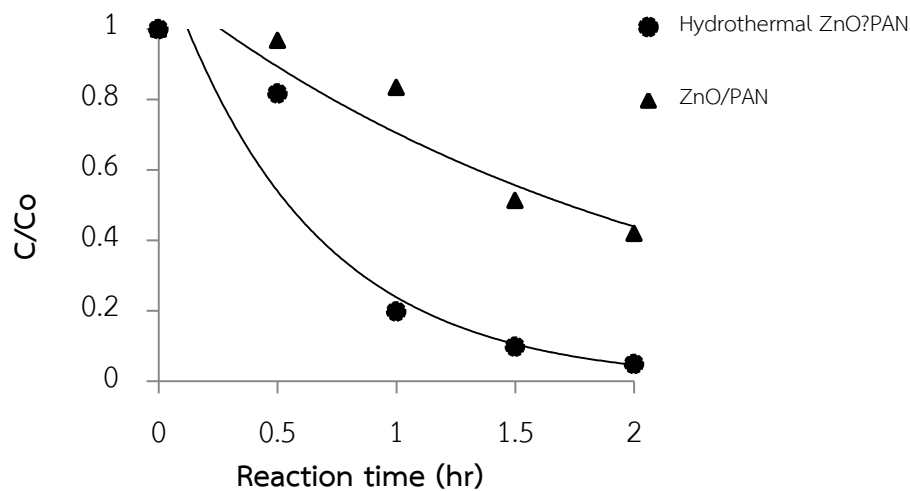


Fig. 32 photocatalytic degradation of toluene in batch reactor by ZnO/PAN nanofibers before and after hydrothermal treatment.

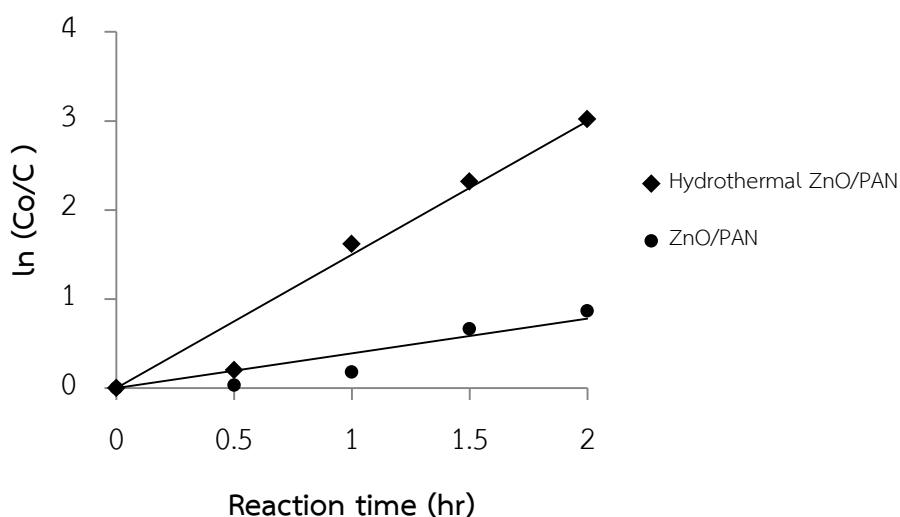


Fig. 33 plot of  $\ln(1/(1-X))$  against reaction time

#### 4.3.1 Effect of zinc acetate concentration

Concentration of zinc acetate could influence ZnO loading as parameter affecting to performance of toluene degradation. It was found that ZnO loading could be increased by increase zinc acetate concentration as Fig. 19. The

ZnO loading was rapidly increased from 13 to 23 and 48% when zinc acetate concentration increase from 0.03 to 0.06 and 0.12 M respectively. The ZnO/PAN nanofibers prepared by various zinc acetate concentration were subjected to remove toluene. Fig. 34 shows photocatalytic degradation of toluene by ZnO/PAN nanofibers prepared by various zinc acetate concentration. It was found that toluene concentration decrease to 4, 2, and 1% within 2 hrs as ZnO/PAN nanofibers prepared by 0.03, 0.06, and 0.12 M zinc acetate concentration were utilized in the process respectively. It was found that toluene was increasingly removed as ZnO/PAN nanofibers prepared by high zinc acetate concentration were utilized because of their more raised ZnO loading. Although ZnO loading was rapidly increased, the performance of toluene removal was gradually enhanced due to ZnO/PAN nanofibers obtained from high zinc acetate concentration possesses low aspect ratio as showed in Table 7, resulting in high charge carrier recombination rate. High charge carrier recombination rate would inhibit photocatalytic activity. Therefore, high photocatalytic activity is favorable to low charge carrier recombination rate. Wang et al [61] and Zhang et al [62] suggested that larger particle size of semiconductor contribute to low charge carrier recombination rate. However, for this work, ZnO possesses shape of rod therefore it should be described by aspect ratio. Zhang et al [63] suggested that high aspect ratio contribute to reduce charge carrier recombination rate.

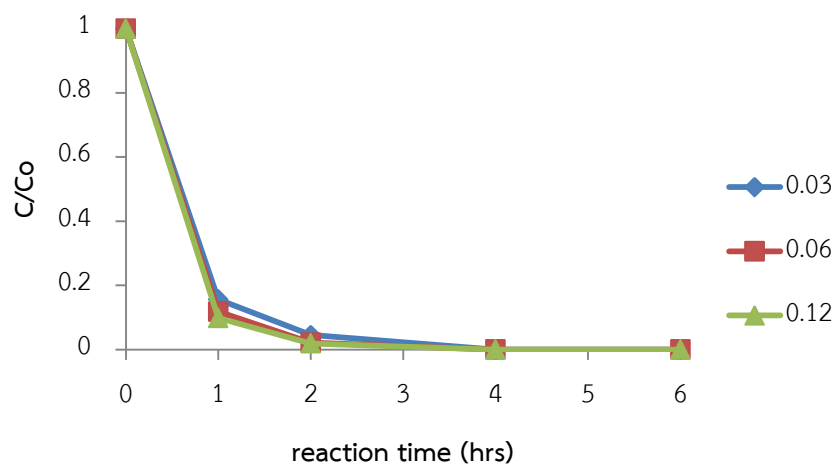


Fig. 34 photocatalytic degradation of toluene in batch reactor by ZnO/PAN nanofibers prepared by various zinc acetate concentration (M).

Table 7. aspect ratios of ZnO nanorods prepared by various zinc acetate concentrations

zinc acetate concentration (M)	aspect ratio
0.03	9.2
0.06	5.2
0.12	3.0

#### 4.3.1 Effect of temperature

Photocatalyst loading and aspect ratio were considered as important parameters to performance of photocatalytic reaction. Preparation of ZnO/PAN nanofibers by hydrothermal treatment could influence these parameters. Hydrothermal temperature is one of important factor. Increase of hydrothermal temperature contributes to increase ZnO loading as Fig. 22. Therefore, increase of hydrothermal temperature was expected to enhance performance of toluene

removal because of increased ZnO loading. Fig. 35 shows the photocatalytic degradation of toluene by ZnO/PAN nanofibers prepared by various hydrothermal temperatures. It was found that concentration of toluene decrease by times. The concentration of toluene remains in the reactors for 11, 3, and 3% when ZnO/PAN nanofibers prepared by 100, 140, and 180°C hydrothermal temperature were used in the processes respectively. It was found that the gaseous toluene was increasingly removed as ZnO/PAN nanofibers prepared by high hydrothermal temperature were used. The ZnO/PAN nanofibers prepared by higher hydrothermal temperature contribute to higher performance of toluene removal because of more ZnO loading. Moreover, ZnO nanorods prepared by higher temperature possess high aspect ratio as showed in Table 8 therefore it encourages high performance of toluene removal as above reasons. Although ZnO nanorods prepared at 100°C possess aspect ratio is higher than 140°C, loading of ZnO is lower. Therefore, it could be claimed that ZnO loading is the parameter that is more important than the aspect ratio.

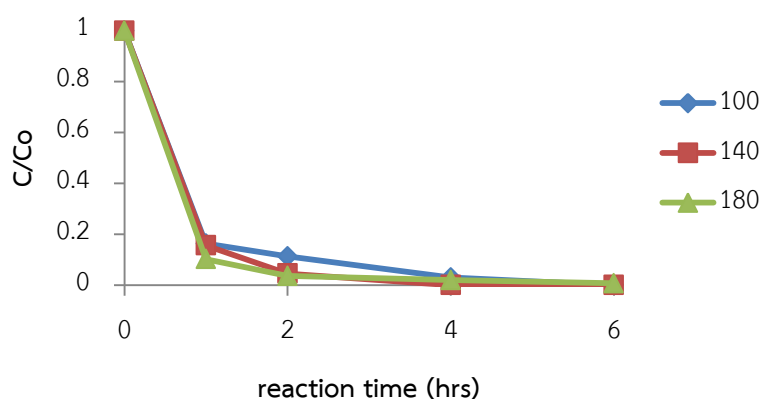


Fig. 35 photocatalytic degradation of toluene in batch reactor by ZnO/PAN nanofibers prepared by various hydrothermal temperatures (°C).

Table 8. aspect ratios of ZnO nanorods prepared by various hydrothermal temperatures

temperature (°C)	aspect ratio
100	8.7
140	5.2
180	19.5

#### 4.3.1 Effect of treatment time

Hydrothermal treatment time was expected to influence ZnO loading and surface area, but Fig. 25 shows that the varied treatment times could not significantly influence ZnO loading. Therefore, performance of toluene removal was expected that is not different. Fig. 36 shows the photocatalytic degradation of toluene by ZnO/PAN nanofibers prepared by various treatment times. It was found that is almost the same line. Therefore, ZnO/PAN nanofibers prepared by various treatment times could not influence performance of toluene removal due to ZnO loading were almost equal.

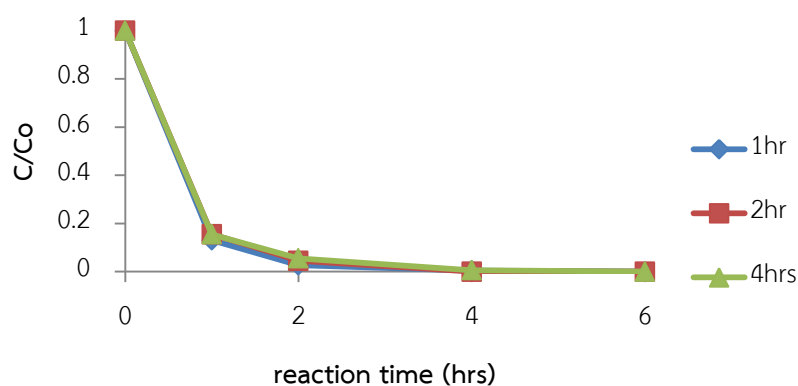


Fig. 36 photocatalytic degradation of toluene in batch reactor by ZnO/PAN nanofibers prepared by various treatment times.

## Chapter V

### Conclusion

#### 5.1 Summary of results

ZnO seeds uniformly embed on PAN nanofibers could be prepared by electrospinning technique of suspension of ZnO and PAN. Average diameter of electrospun nanofibers is 317 nm. ZnO nanorods could be grown on the surface of PAN nanofibers by hydrothermal treatment using zinc acetate and HMT as precursor where ZnO seeds act as nucleation sites. Therefore, the fibers like tube-brush were obtained. Presence of ZnO in the fibers could increase specific surface area. Meanwhile, the fibers undergone hydrothermal treatment could be obtained higher specific surface area.

Increase of zinc acetate concentration contributes to obtain larger diameter of ZnO nanorods and higher ZnO loading. 0.02 M zinc acetate concentration could contribute to obtained highest diameter of 131 nm. Increase of hydrothermal temperature could significantly increase length of ZnO nanorods and ZnO loading. Highest of ZnO nanorods length of 1184 nm could be obtained by hydrothermal treatment at 180°C. Extending treatment times in the period of 1-4 hrs could not influence on length and diameter of ZnO nanorods and ZnO loading. Zinc



acetate:HMT ratio of 1:1 is the optimal ratio to obtain ZnO/PAN nanofibers without residual reactants.

The ZnO/PAN nanofibers prepared by hydrothermal treatment still possess flexibility. Hydrothermal treatment could increase tensile modulus and higher treatment temperature contributes the fibers to have higher tensile modulus. Presence of ZnO in the fibers could enhance performance of toluene removal. Moreover, ZnO/PAN nanofibers obtained by hydrothermal treatment could remove toluene is better than ZnO seeds/PAN nanofibers. Gaseous toluene could be completely removed within 2 hrs in batch reactor using ZnO/PAN nanofibers prepared by hydrothermal treatment. Increase of concentration of zinc acetate and treatment temperature contributes the fibers to have higher performance of toluene removal.

## 5.2. Conclusion

Flexible ZnO/PAN nanofibers could be successfully prepared by electrospinning technique combined with hydrothermal treatment. The ZnO/PAN nanofibers possess morphology like tube-brush. Increase of zinc acetate concentration and treatment temperature could increase diameter and length of ZnO nanorods respectively, resulting in larger ZnO loading. Treatment time varied in the experiment could not influence on dimension of ZnO and ZnO loading. Zinc acetate:HMT ratio of 1:1 is the optimal ratio to obtain ZnO/PAN. ZnO/PAN

nanofibers obtained by hydrothermal treatment have higher performance of toluene removal.

### 5.3 Recommendations for future work

Some recommendations for study in the future were given as below.

1. The interaction between ZnO and PAN nanofibers should be investigated such as physical or chemical interaction.
2. Degradation of gaseous toluene under continuous reactor should be studied.
3. Degradation of PAN nanofibers after photocatalytic process should be studied.



## REFERENCES

- [1] Mo, J.;Zhang, Y.;Xu, Q.;Lamson, J.J.;Zhao, R., *Atmospheric Environment*, **43**, 2229-2246 (2009)
- [2] Zhan, S.;Yang, Y.;Gao, X.;Yu, H.;Yang, S.;Zhu, D.;Li, Y., *Catalysis Today*, **225**, 10-17 (2014)
- [3] Sayama, K.;Hayashi, H.;Arai, T.;Yanagida, M.;Gunji, T.;Sugihara, H., *Applied Catalysis B: Environmental*, **94**, 150-157 (2010)
- [4] Dan Li, Y.W., and Younan Xia, *Nano Letters*, **3**, 1167-1171 (2003)
- [5] Watthanaarun, J.;Pavarajarn, V.;Supaphol, P., *Science and Technology of Advanced Materials*, **6**, 240-245 (2005)
- [6] Tekmen, C.;Suslu, A.;Cocen, U., *Materials Letters*, **62**, 4470-4472 (2008)
- [7] Park, J.-A.;Moon, J.;Lee, S.-J.;Lim, S.-C.;Zyung, T., *Current Applied Physics*, **9**, S210-S212 (2009)
- [8] Kim, S.;Lim, S.K., *Applied Catalysis B: Environmental*, **84**, 16-20 (2008)
- [9] Wang, B.;Chen, Z.;Zhang, J.;Cao, J.;Wang, S.;Tian, Q.;Gao, M.;Xu, Q., *Colloids and Surfaces A: Physicochemical and Engineering Aspects*, **457**, 318-325 (2014)
- [10] Sangkhaprom, N.;Supaphol, P.;Pavarajarn, V., *Ceramics International*, **36**, 357-363 (2010)
- [11] Su, C.;Ran, X.;Hu, J.;Shao, C., *Environmental science & technology*, **47**, 11562-11568 (2013)
- [12] Lu, C.-H.;Yeh, C.-H., *Ceramics International*, **26**, 351-357 (2000)
- [13] Polsongkram, D.;Chamnink, P.;Pukird, S.;Chow, L.;Lupan, O.;Chai, G.;Khallaf, H.;Park, S.;Schulte, A., *Physica B: Condensed Matter*, **403**, 3713-3717 (2008)
- [14] Zhou, Y.;Li, D.;Zhang, X.;Chen, J.;Zhang, S., *Applied Surface Science*, **261**, 759-763 (2012)
- [15] Li, H.;Jiao, S.;Li, H.;Li, L., *Journal of Materials Science: Materials in Electronics*, **25**, 2569-2573 (2014)
- [16] Alver, Ü.;Tanrıverdi, A.;Akgül, Ö., *Synthetic Metals*, **211**, 30-34 (2016)

- [17] Ji, L.-W.;Peng, S.-M.;Wu, J.-S.;Shih, W.-S.;Wu, C.-Z.;Tang, I.T., *Journal of Physics and Chemistry of Solids*, **70**, 1359-1362 (2009)
- [18] Solis-Pomar, F.;Martinez, E.;Melendrez, M.F.;Perez-Tijerina, E., *Nanoscale research letters*, **6**, 524 (2011)
- [19] Lim, J.-H.;Ryu, J.-Y.;Moon, H.-S.;Kim, S.-E.;Choi, W.-C., *Transactions on Electrical and Electronic Materials*, **13**, 305-309 (2012)
- [20] Öztürk, S.;Kılınç, N.;Taşaltın, N.;Öztürk, Z.Z., *Physica E: Low-dimensional Systems and Nanostructures*, **44**, 1062-1065 (2012)
- [21] Song, J.;Baek, S.;Lim, S., *Physica B: Condensed Matter*, **403**, 1960-1963 (2008)
- [22] Ongwandee, M.;Moonrinta, R.;Panyametheekul, S.;Tangbanluekal, C.;Morrison, G., *Building and Environment*, **46**, 1512-1522 (2011)
- [23] **4**, 191-215 (Ulmann)
- [24] Simonsen, M.E., 135-170 (2014)
- [25] Pawar, R.C.;Lee, C.S., 1-23 (2015)
- [26] Morkoç, H.;Özgür, Ü., General Properties of ZnO, Zinc Oxide, Wiley-VCH Verlag GmbH & Co. KGaA2009, pp. 1-76.
- [27] Pearton, S., *Progress in Materials Science*, **50**, 293-340 (2005)
- [28] Kołodziejczak-Radzimska, A.;Jesionowski, T., *Materials*, **7**, 2833 (2014)
- [29] Byrappa, K.;Adschiri, T., *Progress in Crystal Growth and Characterization of Materials*, **53**, 117-166 (2007)
- [30] "Molecular Thermodynamics of Complex Systems, Springer Berlin Heidelberg, 2009.
- [31] Bhardwaj, N.;Kundu, S.C., *Biotechnology advances*, **28**, 325-347 (2010)
- [32] Frenot, A.;Chronakis, I.S., *Current Opinion in Colloid & Interface Science*, **8**, 64-75 (2003)
- [33] Huang, Z.-M.;Zhang, Y.Z.;Kotaki, M.;Ramakrishna, S., *Composites Science and Technology*, **63**, 2223-2253 (2003)
- [34] Nataraj, S.K.;Yang, K.S.;Aminabhavi, T.M., *Progress in Polymer Science*, **37**, 487-513 (2012)
- [35] Wypych, G., PAN polyacrylonitrile, Handbook of Polymers (Second Edition), ChemTec Publishing2016, pp. 271-275.

- [36] Drew, C.;Liu, X.;Ziegler, D.;Wang, X.;Bruno, F.F.;Whitten, J.;Samuelson, L.A.;Kumar, J., *Nano Letters*, **3**, 143-147 (2003)
- [37] Xu, J.;Shi, S.;Wang, C.;Zhang, Y.;Liu, Z.;Zhang, X.;Li, L., *Journal of Alloys and Compounds*, **648**, 521-526 (2015)
- [38] Tonto, P.;Mekasuwandumrong, O.;Phatanasri, S.;Pavarajarn, V.;Praserthdam, P., *Ceramics International*, **34**, 57-62 (2008)
- [39] Thangavel, R.;Chang, Y.-C., *Thin Solid Films*, **520**, 2589-2593 (2012)
- [40] Schlur, L.;Carton, A.;Lévêque, P.;Guillon, D.;Pourroy, G., *The Journal of Physical Chemistry C*, **117**, 2993-3001 (2013)
- [41] Chen, Y.-Y.;Kuo, C.-C.;Chen, B.-Y.;Chiu, P.-C.;Tsai, P.-C., *Journal of Polymer Science Part B: Polymer Physics*, **53**, 262-269 (2015)
- [42] Kayaci, F.;Vempati, S.;Ozgit-Akgun, C.;Biyikli, N.;Uyar, T., *Applied Catalysis B: Environmental*, **156-157**, 173-183 (2014)
- [43] Tang, F.;Yang, X., *Building and Environment*, **56**, 329-334 (2012)
- [44] Pei, C.C.;Leung, W.W.-F., *Applied Catalysis B: Environmental*, **174-175**, 515-525 (2015)
- [45] Krishnan;J.;Swaminathan;T., *Latin American applied research*, (2010)
- [46] Jo, W.K.;Kang, H.J., *Journal of hazardous materials*, **283**, 680-688 (2015)
- [47] Wang, S.-F.;Tseng, T.-Y.;Wang, Y.-R.;Wang, C.-Y.;Lu, H.-C., *Ceramics International*, **35**, 1255-1260 (2009)
- [48] Li, H.;Jiao, S.;Bai, S.;Li, H.;Gao, S.;Wang, J.;Yu, Q.;Guo, F.;Zhao, L., *Phys. Status Solidi A*, **211**, 595-600 (2014)
- [49] Tsai, J.-K.;Meen, T.-H.;Wu, T.-C.;Lai, Y.-D.;He, Y.-K., *Microelectronic Engineering*, **148**, 55-58 (2015)
- [50] Wang, M.;Ye, C.-H.;Zhang, Y.;Hua, G.-M.;Wang, H.-X.;Kong, M.-G.;Zhang, L.-D., *Journal of Crystal Growth*, **291**, 334-339 (2006)
- [51] Zou, X.;Fan, H.;Tian, Y.;Yan, S., *Materials Letters*, **107**, 269-272 (2013)
- [52] Li, W.-J.;Shi, E.-W.;Zhong, W.-Z.;Yin, Z.-W., *Journal of Crystal Growth*, **203**, 186-196 (1999)
- [53] Fang, M.;Liu, Z.W., *Ceramics International*, **43**, 6955-6962 (2017)
- [54] Zhou, Z.;Deng, Y., *The Journal of Physical Chemistry C*, **113**, 19853-19858 (2009)

- [55] Cheng, S.L.;Syu, J.H.;Liao, S.Y.;Lin, C.F.;Yeh, P.Y., *RSC Adv.*, **5**, 67752-67758 (2015)
- [56] Ravandi, S.A.H.;Sadrajahani, M., *Journal of Applied Polymer Science*, **124**, 3529-3537 (2012)
- [57] Jeong, J.;Sekiguchi, K.;Lee, W.;Sakamoto, K., *Journal of Photochemistry and Photobiology A: Chemistry*, **169**, 279-287 (2005)
- [58] Zhao, J.;Yang, X., *Building and Environment*, **38**, 645-654 (2003)
- [59] Saucedo-Lucero, J.O.;Arriaga, S., *Chemical Engineering Journal*, **218**, 358-367 (2013)
- [60] Tejasvi, R.;Sharma, M.;Upadhyay, K., *Chemical Engineering Journal*, **262**, 875-881 (2015)
- [61] Wang, C.-C.;Zhang, Z.;Ying, J.Y., *Nanostructured Materials*, **9**, 583-586 (1997)
- [62] Zhang, Z.;Wang, C.C.;Zakaria, R.;Ying, J.Y., *J. Phys. Chem. B*, **102**, 10871-10878 (1998)
- [63] Zhang, X.;Qin, J.;Xue, Y.;Yu, P.;Zhang, B.;Wang, L.;Liu, R., *Scientific reports*, **4**, 4596 (2014)





## ZNO/PAN NANO FIBERS AFTER HYDROTHERMAL TREATMENT

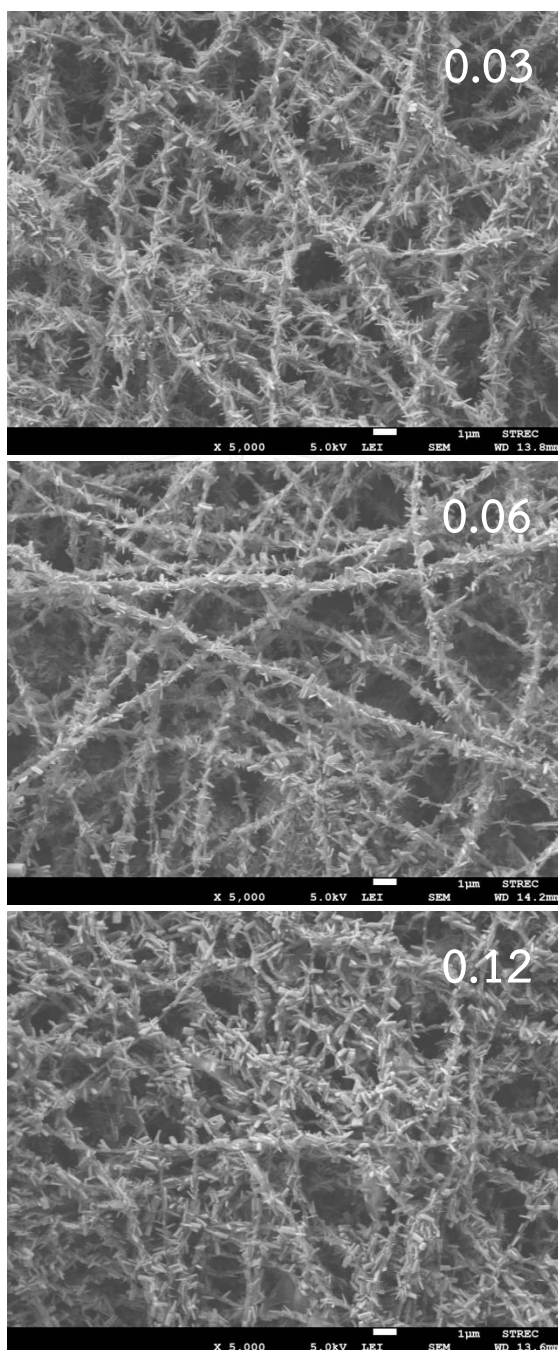


Fig. 37 SEM images of ZnO/PAN nanofibers prepared by various zinc acetate concentrations (M).



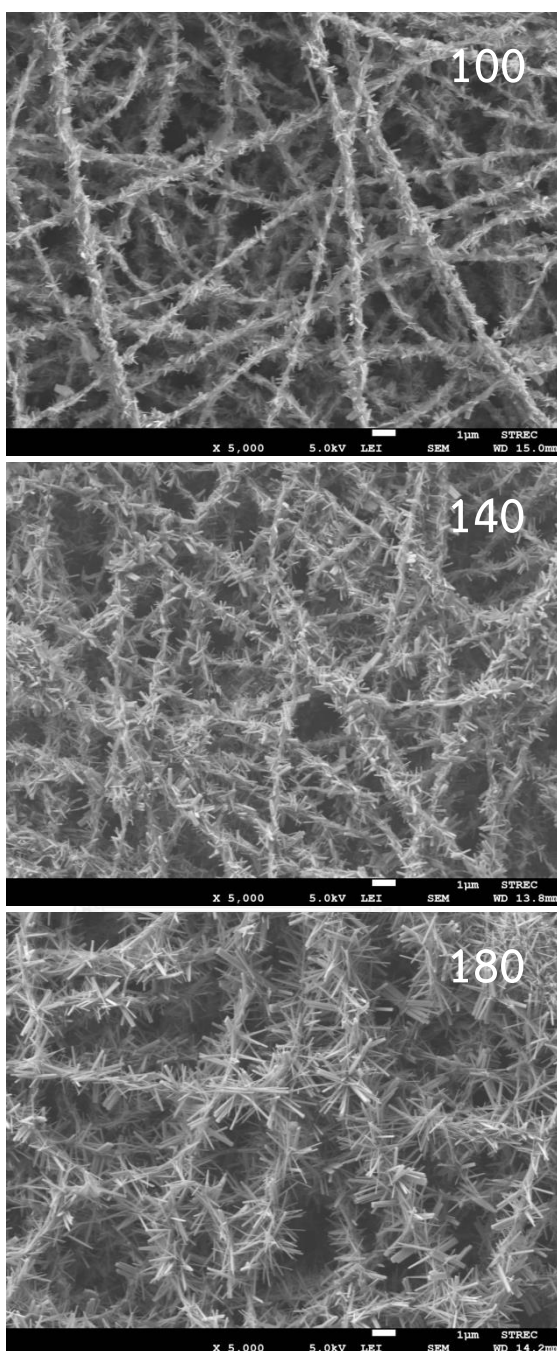


Fig. 38 SEM images of ZnO/PAN nanofibers prepared by various treatment temperatures ( $^{\circ}\text{C}$ ).

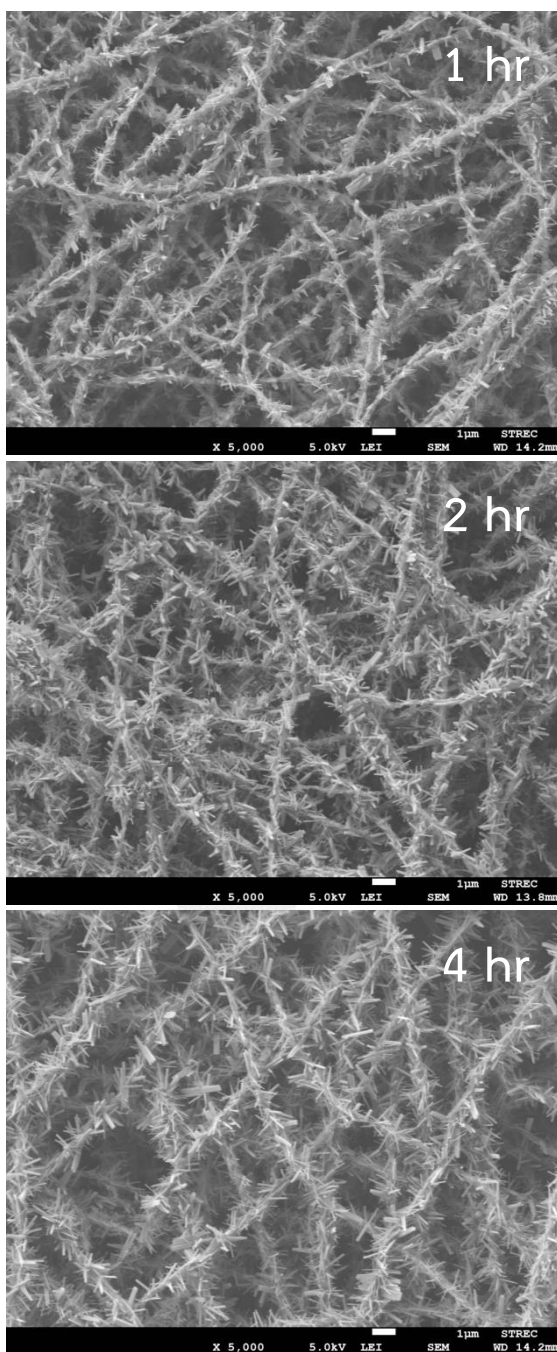


Fig. 39 SEM images of ZnO/PAN nanofibers prepared by various treatment time.

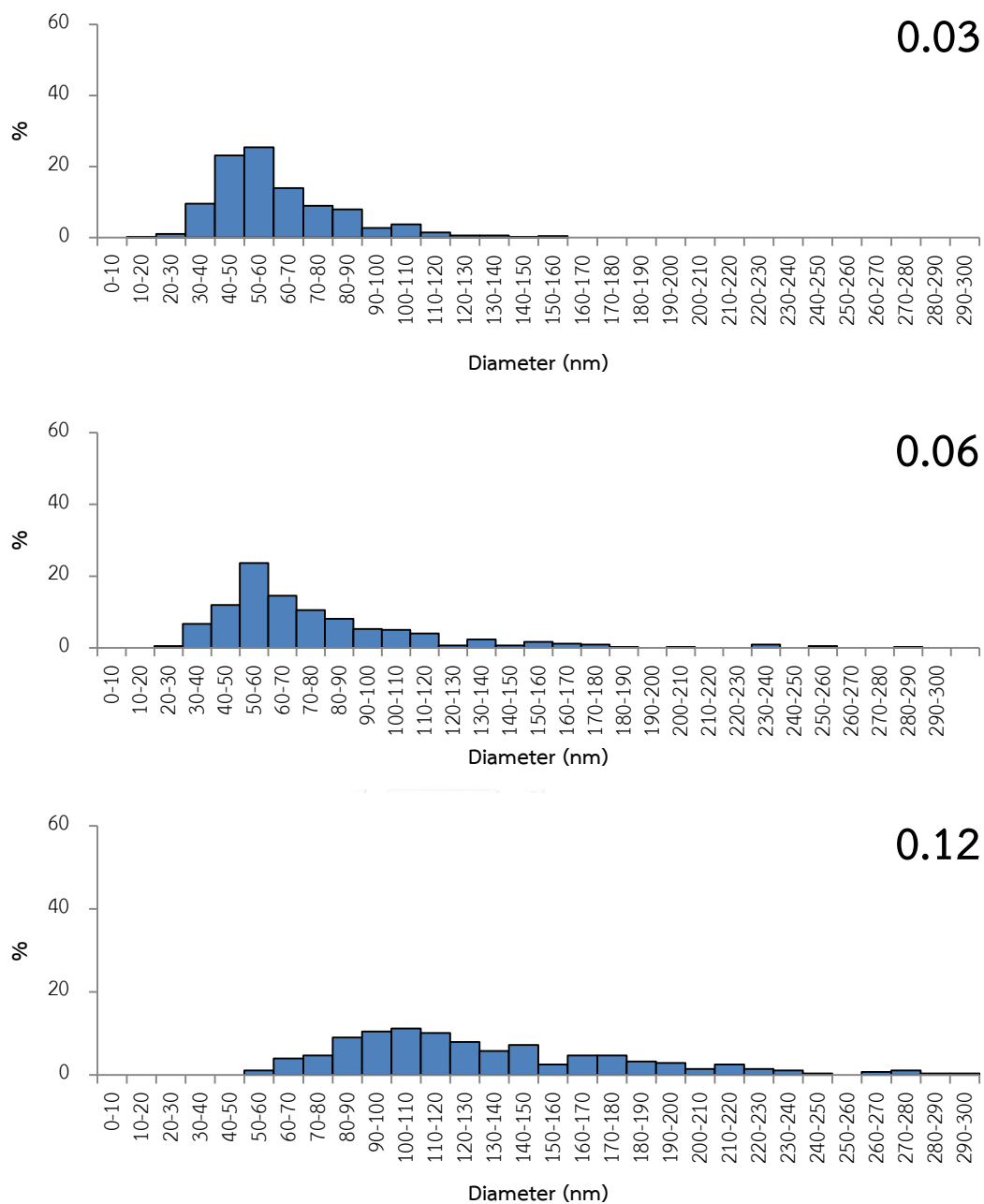


Fig. 40 diameter size distribution of ZnO nanorods prepared by various zincacetate concentrations (M).

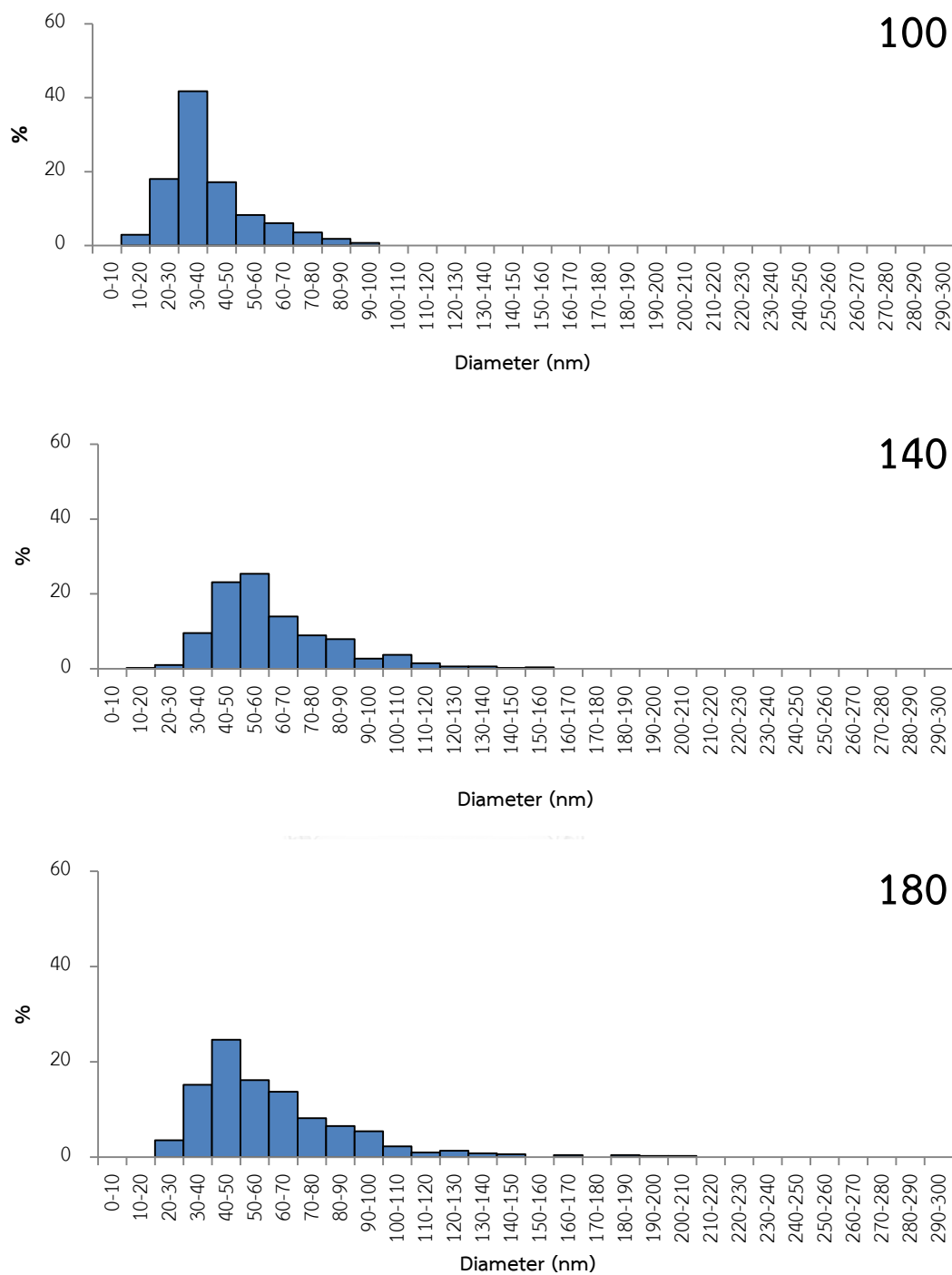


Fig. 41 diameter size distribution of ZnO nanorods prepared by treatment temperatures ( $^{\circ}\text{C}$ ).

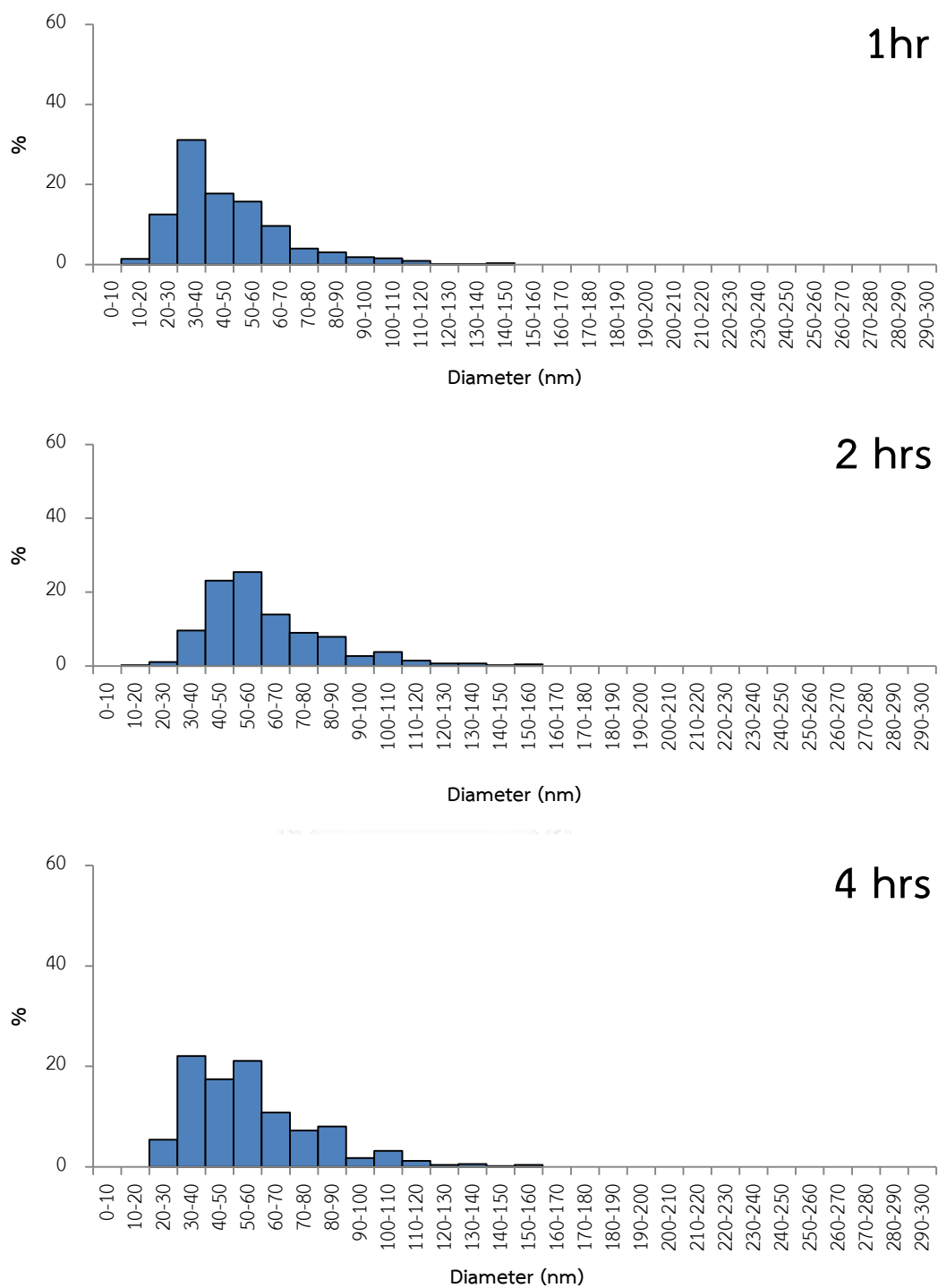


Fig. 42 diameter size distribution of ZnO nanorods prepared by treatment times.

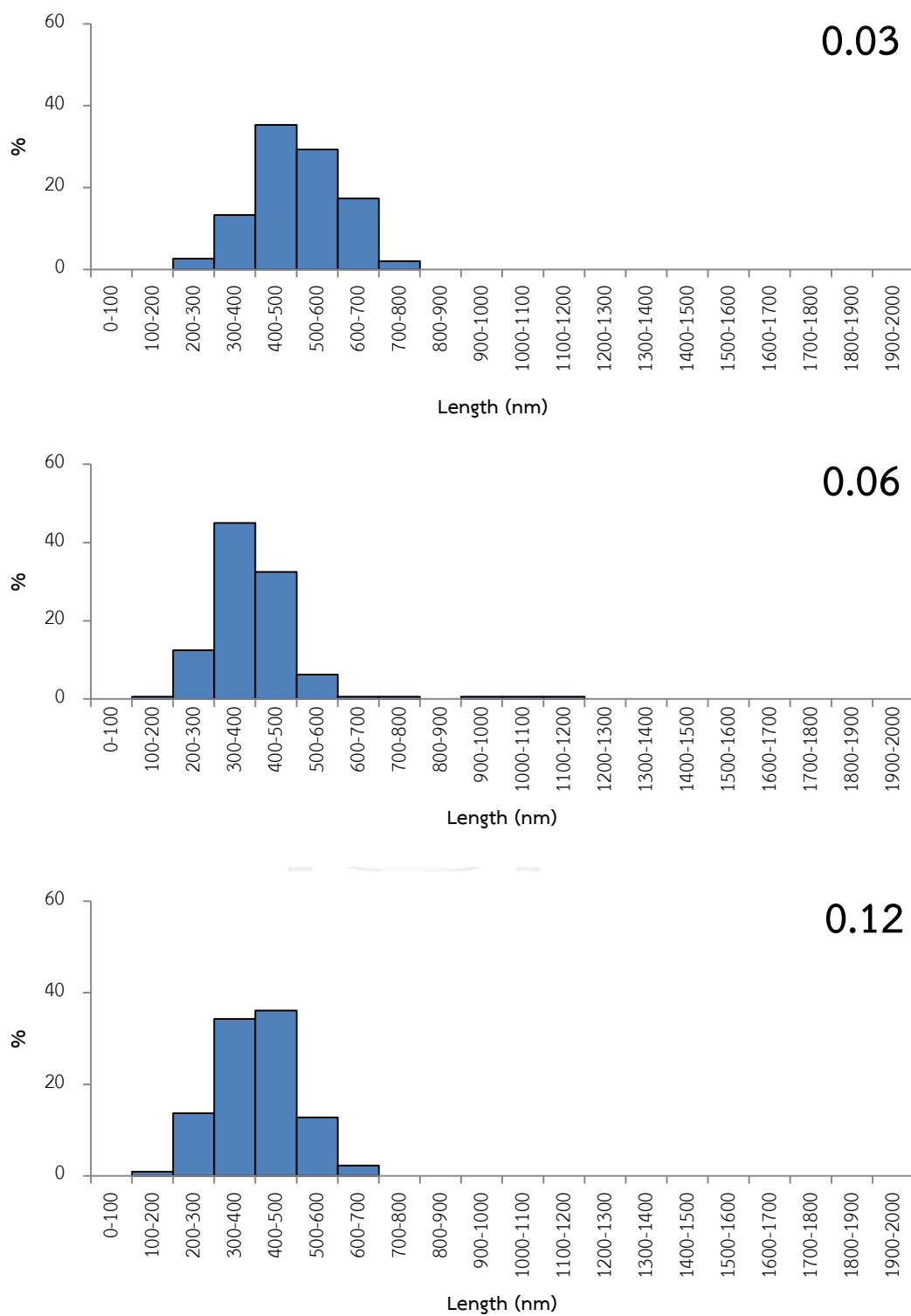


Fig. 43 length size distribution of ZnO nanorods prepared by various zincacetate concentrations (M).

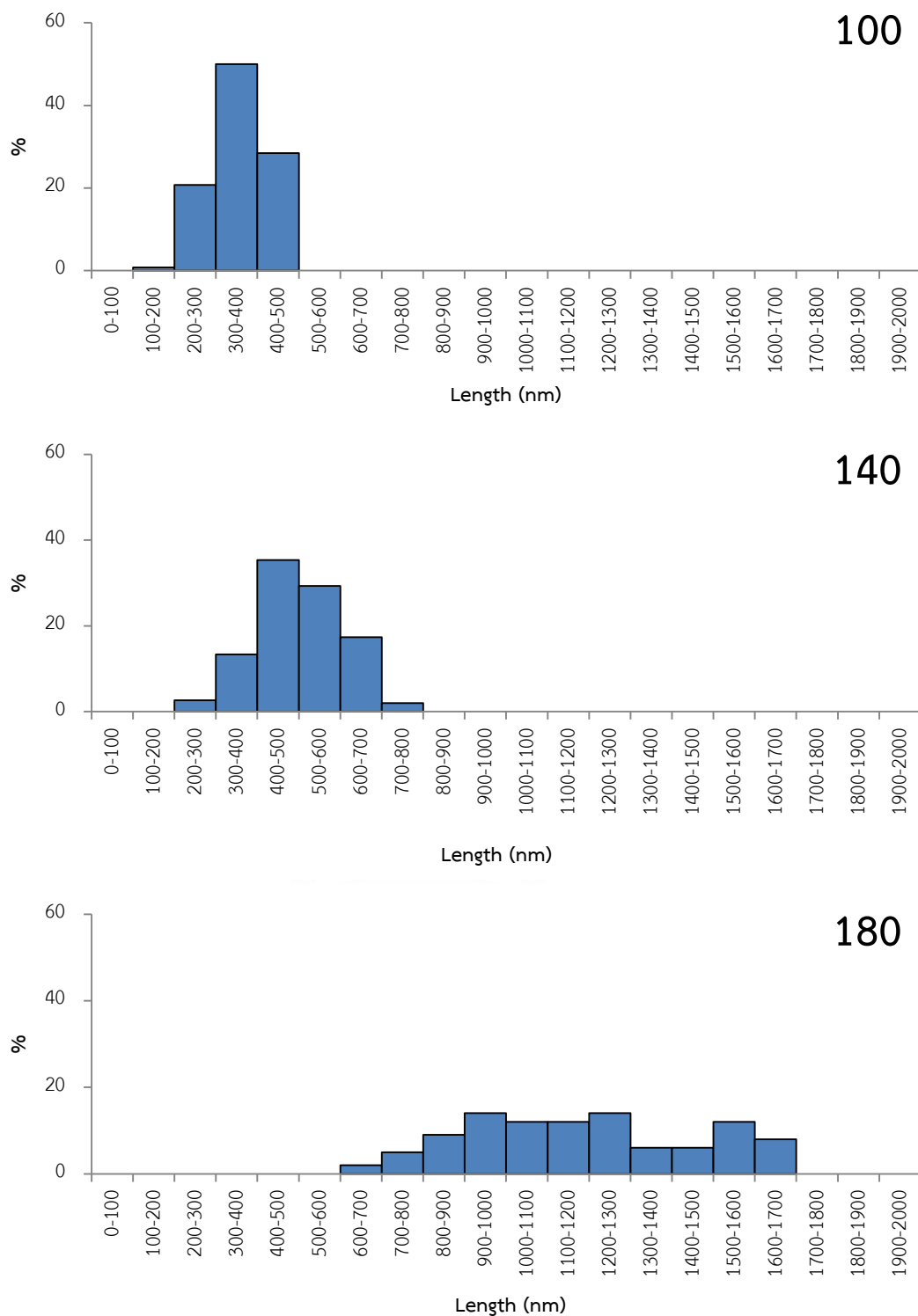


Fig. 44 length size distribution of ZnO nanorods prepared by treatment temperatures ( $^{\circ}$ C).

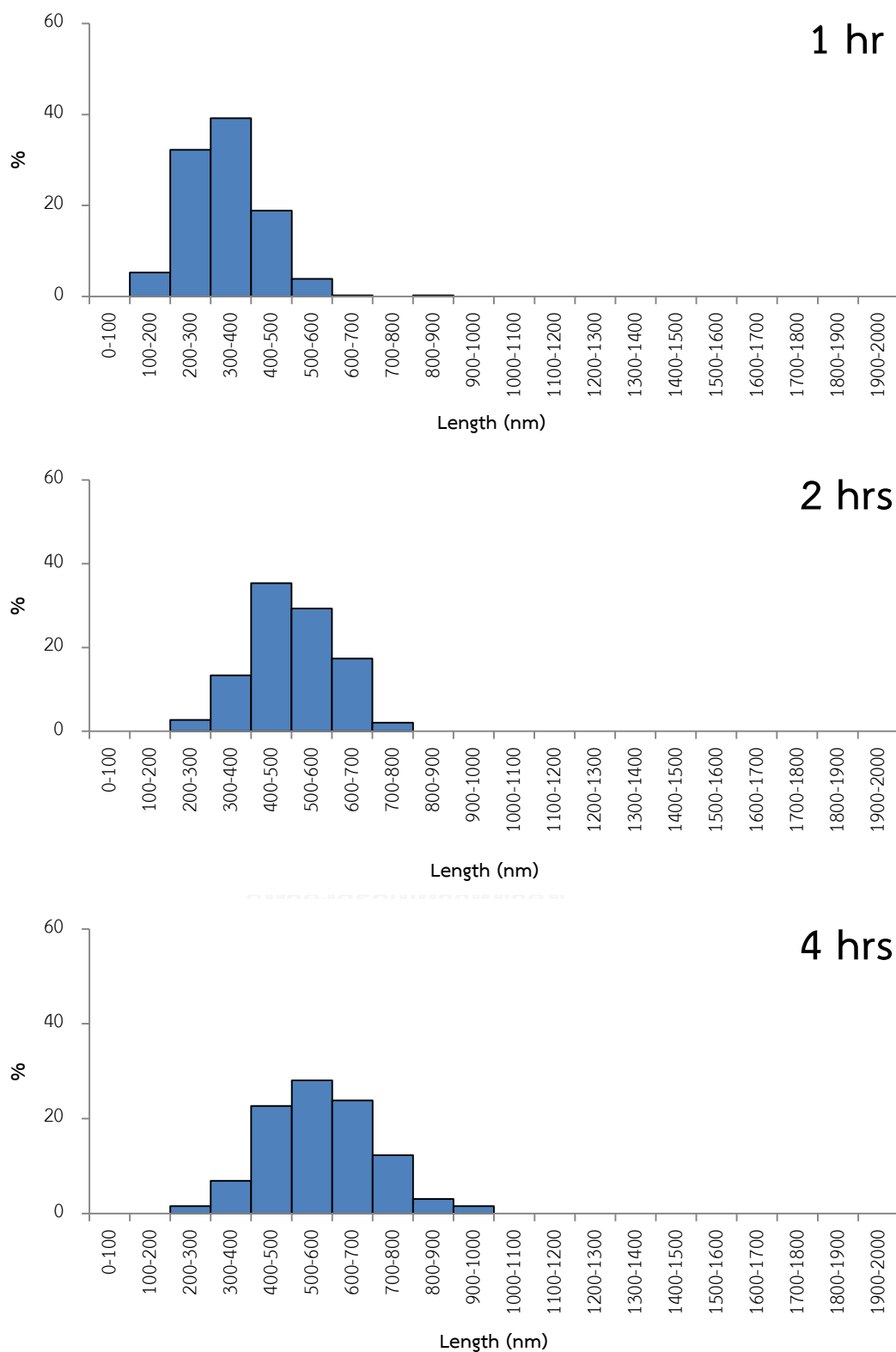


Fig. 45 length size distribution of ZnO nanorods prepared by treatment times.



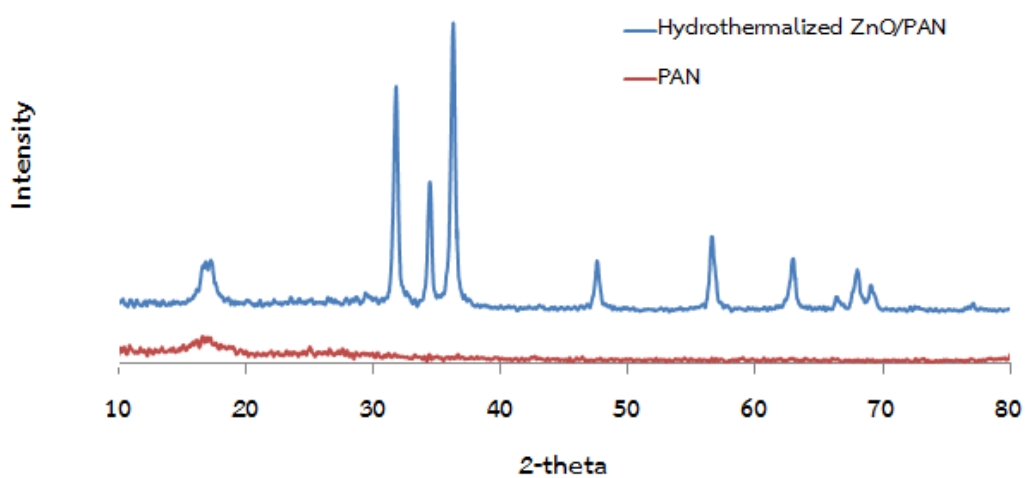


Fig. A46 XRD pattern of PAN and ZnO/PAN nanofibers.

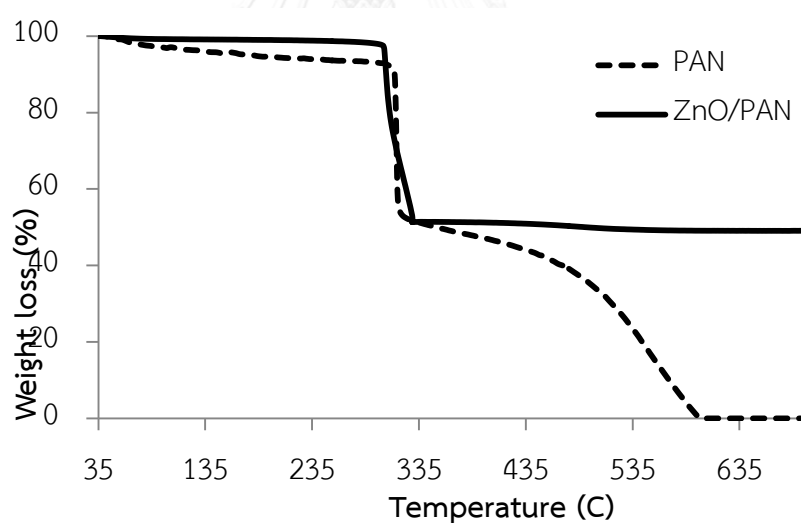


Fig. 47 TGA curve of PAN and ZnO/PAN nanofibers

## VITA

Mr. Wuttichai Manoi was born on 30 May, 1991, in Sukhothai, Thailand. He received a graduated Bachelor Degree of Engineering in the major of chemical engineering from Naresuan University. He continued to study in Master Degree of Chemical Engineering, Faculty of Engineering, Chulalongkorn University.

